Universidade do Minho
Escola de Engenharia

Sílvia Manuela Ferreira da Cruz

Characterization of Nano-Reinforced Thermoplastic Elastomers

Abril de 2009

Universidade do Minho
Escola de Engenharia

Sílvia Manuela Ferreira da Cruz

Characterization of Nano-Reinforced Thermoplastic Elastomers

Dissertação de Mestrado
Área de Especialização Processamento e Caracterização de Materiais

Trabalho efectuado sob a orientação do
Professor Doutor Júlio César Machado Viana

Abril de 2009

ACKNOWLEDGEMENTS

The author would like to extend his gratitude to the following individuals and institutions for their valuable contribution in the completion of this thesis:

Prof. Júlio C. Viana, research and scientific supervisor, for the continuous support and availability, the scientific guidance and the friendly encouragements in which all contributed to the coherence and value-added scientific reached. I hope to be and continue meritorious of his unconditional trust.

The Hosting institutions: Innovation in Polymers Engineering (Pólo de Inovação Engenharia de Polímeros, PIEP) and the Polymer Engineering Department (Departamento de Engenharia de Polímeros, DEP) of the University of Minho for the facilities and equipment provided for this research.

The technical staff: Mrs Paula Peixoto from PIEP, Mr. Mauricio Malheiro, Mr. Serafim Sampaio, Mr. Francisco Mateus, and Mr. Manuel Escourido from DEP, for their help with the experimental work.

Professor Dr. Senentxu Lanceros-Mendez and Pedro Costa from Physics Department for the help on the resistivity tests presented on this work.

All my researcher (just colleagues) colleagues at PIEP and DEP for their direct and indirect contribution for this work as well as for their friendly acceptance and support.

I gratefully acknowledge to the financial support of the European Commission under the sixth FP6 within the CEC-made-shoe project (ISTNMP 2004-507378).

Finally to those who gave me their ultimate support, patience and incentive: my Family.

Sílvia Cruz

Guimarães, April 2009

SUMÁRIO

Os Termoplásticos elastómeros, TPEs, têm vindo a substituir os tradicionais elastómeros devido à sua elevada eficiência mecânica, à sua alta processabilidade e baixo custo. Numa gama cada vez mais alargada de aplicações (p.e., nas indústrias automóvel e militar, componentes médicos, electrónica, construção civil, etc.) as exigências aumentam, assim como a necessidade de materiais com propriedades melhoradas. A mistura de um polímero com um outro material dá origem a um novo sistema polimérico com propriedades melhoradas, resultante da combinação das propriedades existentes. A incorporação de reforços no TPE poderá adicionar-lhe novas funcionalidades e apresentar melhoramentos quanto ao seu desempenho. Os compósitos de TPEs a estudar, incorporarão reforços de escala micro e nanométrica. Dois tipos de TPEs serão considerados pela sua natureza: amorfo-amorfo (p.e. SBS) e amorfo-semicristalino (p.e. TPU). Isto permitirá induzir diferentes estados morfológicos e investigar a relevância das interacções interfásicas. Reforços como negro de fumo, nanofibras de carbono, nanosilica, nanoclays e vermiculites têm despertado grande interesse pelas propriedades que exibem. A combinação destes com os TPE pode resultar em materiais com melhores propriedades e "inteligentes" que podem ser integrados em sistemas como sensores/controladores de deformação ou força, temperatura, etc. O desenvolvimento destes compósitos requer um certo know-how. Não é certo que adição destes reforços irá conferir as funcionalidades desejadas, mais ainda quando feito com percentagens de incorporação muitos baixas e de difícil dispersão. Será um compromisso entre vários critérios que influenciarão desde a sua processabilidade, o seu comportamento mecânico e a sua estabilidade a longo prazo.

Este trabalho tem como principal objectivo caracterizar e compreender o comportamento (mecânico, térmico, eléctrico e ao fogo) dos TPEs carregados com partículas micro e nanométricas.

ABSTRACT

Thermoplastic elastomers, TPEs, have been used to replace the traditional elastomers due to their high mechanical efficiency, easy processabillity and low cost. In an increasingly broad range of applications (e.g., automobile industry and military, medical component, electronics, civil construction, etc.), the demands increases as well as the need for materials with improved and multifunctional properties. The combination of a polymer with a filler gives rise to a new polymer system with improved performance and added functionalities as a result of the combination of the existing properties. The TPE's composites selected for this study will incorporate micro- and nanometric scale reinforcements. Two types of TPEs will be considered for their nature: amorphous-amorphous (e.g. SBS) and amorphous-semicrystalline (e.g. TPU). This will lead to induce different morphological states and investigate the relevance of interfaces interactions. Reinforcements such as carbon black, carbon nanofibers, nanosilica, nanoclays and vermiculites (VC) have attracted great interest due to the properties that they exhibit. The combination of these materials with the TPE may result in high performance and "intelligent" materials, ideal to be integrated in systems like deformability or temperature sensors/controllers, that are able to adapt and response in different applications depending on environmental changes, among others. The development of these composites requires specific know-how. It is not certain that the addition of this reinforcements will grant the desired functionalities, even more when it is used with very low incorporation percentage and of difficult dispersion. It will be a commitment between different criterions that will influence their processability, their mechanical behavior and their long a long term stability.

This work has as main objective the characterization and the understanding of the behavior (mechanical, thermal, electric and to flame) of the reinforced TPE's with micro and nanometrics particles.

TABLE OF CONTENTS

CHAPTER 3: MOTIVATION AND OBJECTIVES

CHAPTER 4: MATERIALS, EQUIPMENT AND EXPERIMENTAL METHODS

LIST OF FIGURES

CHAPTER 2: LITERATURE REVIEW

CHAPTER 3: MOTIVATION AND OBJECTIVES

CHAPTER 4: MATERIAL, EQUIPMENT AND EXPERIMENTAL METHODS

CHAPTER 5: RESULTS AND DISCUSSIONS

APPENDIX III

APPENDIX IV

LIST OF TABLES

CHAPTER 4: MATERIALS, EQUIPMENT AND EXPERIMENTAL METHODS

CHAPTER 5: RESULTS AND DISCUSSIONS

LIST OF SYMBOLS AND ABBREVIATIONS

Latin symbols

b – Thermal absorptance [$W.m^{-2}s^{1}$]

DTG_{max} - Temperature of the maximum rate of weight loss (°C)

E – Modulus of elasticity (Young's Modulus) (MPa)

h – Sample thickness [mm]

nm – nanometers (10^{-9} m)

Ø –Diameter (mm)

P – Pressure (Pa)

T – Temperature (°C)

T_d - Onset temperature of weight loss (°C)

T_g – Glass Transition (°C)

T_m – Melting temperature (°C)

U_b- Energy ate break (J)

U_y – Yield Energy (J)

Greek symbols

α- Thermal diffusivity [$m^2.s^{-1}$]

ΔH – Enthalpy (J/g)

Δl – Displacement (mm)

ε_b - Strain at break (mm/mm)

ε_y –.Yield strain (mm/mm)

λ – Stretching ratio (MPa)

λ_c – Thermal Conductivity [$W.m^{-1}.k^{-1}$]

μm – micrometer (10^{-6} m)

ρ – Density (g/cm^3)

σ_b – Stress at break (MPa)

σ_y – Yield stress (MPa)

r – Thermal resistance [$W^{-1}.K.m^2$]

ABBREVIATIONS

APAM - Alberta Polymer Asymmetric Minimixer

CNF – Carbon Nanofiber

CVD - Chemical Vapor Deposition

DSC - Differential scanning calorimetry

HS – Hard Segments

HSCB – High Structure Carbon Black

MFI – Melt flow index (g/10 min)

MMT – Montmorillonite

NC- Nanoclay

NS – Nanosilica

°C – Degrees Celsius

OM- Optical microscopy

SBS – Styrene-Butadiene-Styrene

SEM - Scanning electron microscopy

SS – Soft segments

TGA – Thermogravimetric analysis

TPE - Thermoplastic Elastomer

TPU – Thermoplastic Polyurethane

VC – Vermiculite

VCC – Vermiculite crude

VCE – Vermiculite exfoliated

CHAPTER 1

INTRODUCTION

This chapter provides an overview on the TPEs materials and the use of reinforcement particles for properties and performance improvement.

1.1. INTRODUCTION

Thermoplastic elastomers, TPEs, are a class of phase separated block-copolymers which consist of soft rubber-segments (conferring its elastic character) and hard glassy or crystallisable chains segments that act as physical crosslink bonds (and impart stiffness and strength). [1,2] During service, TPE behave as elastomers but, in contrast to the classical elastomers, they can be processed by means of the conventional techniques and equipment utilized for all thermoplastics. This peculiarity of TPE is related to their different type of crosslinking bond in their structures. One of the monomers develops the hard, or crystalline, segment that functions as a thermally stable component (which softens and flows under shear, as opposed to the chemical crosslinks between polymeric chains in a conventional, thermosetting rubber); the other monomer develops the soft or amorphous segment, which contributes the rubbery characteristic. A key attribute of most TPEs is the ability to tailor toughness and large strain elasticity by varying the type of monomers, the ratio of hard/soft fractions and the lengths of the hard and soft segments, so the TPEs have been used in many fields. [3] TPEs exhibit an extraordinary combination of reprocessability, elasticity, toughness, low temperature flexibility and strength at relatively high temperatures that make them ideal candidates for engineering applications requiring excellent high mechanical properties; and broad service temperature range.[4] TPE's are used where conventional elastomers cannot provide the range of physical properties needed in the product: Automobile industry; health; shoes soles, including personal care, packaging, sporting goods, houseware, hardware and electronics.[2] TPE materials have the potential to be recyclable since they can be molded, extruded and reused like plastics, but they have typical elastic properties of rubbers which are not recyclable owing to their thermosetting characteristics. They require lower energy costs for processing, are easy of process. TPE are capable of self-assembling by micro- and nanophases segregation processes, allowing the development of different morphologies [5,6] and hence of new properties (e.g., mechanical behavior, chemical resistance).

World consumption of TPE is around 2,1 million of tons in 2006.[7] Global demand for TPEs is forecast to increase 6.2% per year through 2009, reaching 3.1 million metric tons, according to a study made by the Freedonia Group. [8] From this total, 970 thousand tons correspond to rubbers of SBS (styrene-butadiene-styrene) and 470 thousand tons to olefinic thermoplastic rubbers (TPO), followed by polyurethane thermoplastic rubbers (TPU), vulcanized thermoplastic rubbers (TPV), copolyesther rubbers (COPE) and thermoplastic polyamides. As target of great interest in the past decade, TPEs have become a highly sought class of material for replacement of conventional materials in many applications. [9-12] Automobile industry, consumes 600 thousand tons from the total volume. It is

estimated, that approximately 45kg of the car weight corresponds to the TPE, in the more developed markets, Europe and the United States.

Polymer composites are attractive because of the ability to form new materials with enhanced properties by combining existing components. Synergistic effects also occur, offering new product possibilities. [13] Faced with a growing number of mixtures of polymers with different properties, it is important to study a new class of polymers composites, as a means to further reduce the material cost in competitive markets and achieve a different combination of properties. Modification of TPE through the incorporation of micro- and nanoparticles, embedded in a continuous polymeric matrix known as micro- and nanocomposites. With the incorporation of reinforcing particles, TPEs will have adjustable properties, making them a versatile class of materials more advantageous compared to the thermoplastics and elastomers.

Polymer nanocomposites were first heard in 1990 when Toyota noticed an eminent property enhancement of nylon-6 with the incorporation of a small amount of nanoclay.[14] Such improvements were attributed to the increase of the interfacial area between polymer matrix and the filler when the clay platelets were individually dispersed. In 1998, the montmorillonite (MMT) was introduced for the first time by Wang and Pinnavaia [15,16] demonstrating mechanical properties improvements. In the last decade, research has demonstrated that composites of polymers with MMT and vermiculites often exhibit unexpected properties derived from synergy coming from both phases, such as improving thermal, mechanical and retardant properties of the material.[17-26] This lead to an increase of interest for the use of other particles in the preparation of nano-composites, [27-39] as TPEs. [36,38,40] Lately, nanosized carbon based fillers have focused the attention and interest of the scientific and technological community[41,42] Materials such as high structure carbon black (HSCB) and carbon nanofibers (CNF) dispersed in the polymeric matrix are used as components of electric conductivity, due to its excellent electric [43-46] and mechanical properties. [47] This makes them an excellent application for protection of electromagnetic interference (EMI), for dissipation of static electricity and for absorption of electromagnetic radiation.[48] Materials with low electrical resitivity have extraordinary economical potential. If theses materials have the ability to conduct electrical current without great resistance, enormous quantities of energies could be economized and applications like computer chips small and faster could be developed.

In this work, micro- and nanoparticles were incorporated in TPE matrix by melt blending using a laboratory scale mixer. Within the existing possibilities, two distinct types of TPEs where selected for this study according to their structure and potential application use: i) an amorphous-amorphous BC (e.g., SBS); ii) an amorphous-semicrystalline BC (e.g., TPU). They will allow different structuring capabilities by the incorporation of reinforcing particles. The incorporation of nanoclays (NC) and nanosilicas (NS) aimed to improve TPEs the mechanical properties. HSCB and CNF incorporation was to impart anti-static/electrical and thermal conductivity. NC and crude plus exfoliated vermiculite (VCC and VCE) incorporation aimed to improve flame retardant properties. The relation between morphology and properties were established.

Accomplishing this properties combination resulting from the morphology of nanocomposite is conquer a new opportunity in the conception of polymers responding to stimuli that otherwise wouldn't be possible.

1.2. REFERENCES

1. Holden G., Milkovich R. - Rubberlike block polymers. U.S. Patent 3265765, 1966.
2. Fakirov S. - Handbook of Condensation Thermoplastic Elastomer. 1st ed. WILEY-VCH, 2005.
3. Honeker C.C., Thomas E.L. - Impact of Morphological Orientation in Determining Mechanical Properties in Triblock Copolymer Systems. Chemistry of Materials. Vol. 8: n°8:(1996), p. 1702-1714.
4. Aso O., Eguiazábal J.I., Nazábal J. - The influence of surface modification on the structure and properties of a nanosilica filled thermoplastic elastomer. Composites Science and Technology, Vol. 67: n°13 (2007), p. 2854-2863.
5. Abetz V., Goldacker T., Macromol. Rapid Commun. Vol 21(2000), p.16-34.
6. Matsen M.W., BatesF., - Unifying weak- and strong-segregation block copolymer theories, Macromolecules, Vol.29, p.1091; Origins of complex self-assembly in block copolymers, Macromolecules. Vol.29 (1996), p. 7641.
7. Kear K.E., Developments in Thermoplastic Elastomers. Rapra Technology Limited, 2003.
8. http://www.thefreelibrary.com/TPE+demand+to+reach+3.1+mmt+in+2009-a0143305214.
9. Dutta N.K., Bhowmick A.K., Choudhury N.R. - Handbook of Thermoplastic Elastomers. Olagoke, O., Ed.. Marcel Dekker: New York, 1997. Chapter 15.
10. Bhowmick A.K., De S.K. - Thermoplastic Elastomers from Rubber–Plastic Blends. De, S. K., Bhomwick, A. K., Eds.; Ellis Harwood: New York, 1990. Chapter 1.
11. Utracki L.A., Polymers Engineering Science. Vol. 35: n° 2 (1995).
12. School R.J. - Handbook of Thermoplastic Elastomers. Walker B. M., Rader C. P., Eds.; Van Nostrand Reinhold: New York, 1988. Chapter 9.
13. Breuer O., Sundararaj U., Polymer Composites. Vol. 25:(2004), p. 630.
14. Kojima Y.,Usuki A., Kawasumi M., Fukushima Y., Okada A., Kurauchi T., Kamigaito O. J, Mat. Res. Vol. 8: (1993) p.1185.
15. Zou H., Ran Q., Wu S., Shen J. Polymer Composites. 2008. p.1-5.
16. Wang Z., Pinnavaia T.J.. Chem. Mater. Vol.10 (1998), p.769.
17. Vaia K.H., Giannelis E. P. Macromolecules. Vol.30: (1997), p. 8000.
18. Gârea S. A., Iovu H., Bulearca A. Polymer Testing. Vol. 27 (2008), p.100–113.
19. Cataldo F. Wiley Interscience. Vol. 247(2007), p. 67–77.
20. Lietz S., Yang J., Bosch E., Sandler J. K. W., Zhang Z., Altsta V. Macromolecular Material Engineering. Vol. 292 (2007), p.23–32.
21. Okamoto M., Ray S.S., Prog. Polymer Science. Vol.28 (2003), p.1539.

22. Kornman X., R.T., Mulhaupt R., Finter J., Berglund L. A. Polymer Engineering Science. Vol. 42 (1992), p.1815.
23. Shelley J. S., Matter P.T., DeVries K. L. Polymer. Vol. 42 (2001), p.5849.
24. Kashiwagia T., Harris Jr R.H., Zhang X., Briber R. M., Cipriano B. H.,. Raghavan S. R, Awad W. H., Shields J. R. Polymer. Vol. 45 (2004), p.881.
25. Xu Y., Hoa S.V., Composites Science and Technology. Vol.68 (2008), p.854–861.
26. Kroto H.W., Heath J. R., OBrien S. C., Curl R. F., Smalley R. E. Nature. 1985: p. 318, 162.
27. Rayneud E., Jouen T., Ganthier C., Vigier G., Varlet J. Polymer , 42, 8759 . 2001.
28. Hambir S.,Bulakh N., Kodgire P., Kalgaonkar R., Jog J.P. Journal Polymer Science Part B, Vol. 39 (2001), p.446 17. Ma J., Qi Z., Hu Y. Journal of Applied Polymer Science. Vol. 82 (2001), p. 3611.
29. Ma J.,Qi Z., Hu Y. J App Polym Sci. Vol. 82 (2001), p.3611.
30. Kawasumi M., Hasegawa N., Kato M., Usuki A., Okada A. Macromolecules. Vol.30 (1997), p.6333.
31. Godgire P., Kalgaonkar R., Hambir S., Bulakh N., Jog J.P.. Journal of Applied Polymer Science. Vol. 81 (2001), p.1786.
32. Whang M.Q., Rong M. Z., Zeng H. M., Schmitt S., Wetzel B., Friedrich K. Journal of Applied Polymer Science. Vol.80 (2001), p. 2218.
33. Alexandre M., Debois P., Sun T., Garces J. M., Jérôme R.. Polymer. Vol. 43 (2002), p. 2123.
34. Vu Y.T., Mark J.E., Pham L.H., Engelhardt M. Journal of Applied Polymer Science..Vol. 82 (2001), p.1391 .
35. Ma J., Zang S., Qi Z.. Journal of Applied Polymer Science. Vol. 82 (2001), p.1444.
36. Sadhu S., Bhowmick A. K.. Rubber Chemistry and Technology. Vol. 76 (2003), p.0860.
37. Sadhu S., Bhowmick A. K.. Journal of Applied Polymer Science. Vol. 92 (2004), p. 698.
38. Sadhu S., Bhowmick A. K.. Journal Polymer Science: Polymer Physics. Vol. 42 (2004), p.1573.
39. Donnet J.B., Bansa R.C., Wang M.J. - Carbon Black Science and technology. 2 ed. Revised and extended ed. New York: CRC Press, 1993. 461.
40. Sadhu S., Bhowmick A. K.. Journal of Applied Polymer Science. Vol. 92 (2004), p. 698.
41. Dresselhaus M.S., Dresselhaus G., Eklund P.C.- Science of Fullerenes and Carbon Nanotubes. Academic Press, 1996.
42. Iijima S., Nature.Vol. 56 (1991) p. 354.
43. Strumpler R., Glatz-Reichenbach J.- Conducting Polymer Composites. J. Electroceramics. Vol. 3: n°4 (1999), p.329-346.

44. Feng J., Chan C.M. Polymer Engineering Science. Vol. 43: n° 5 (2003), p.1064-1070.

45. RAMARAJ B. - Electrical and mechanical properties of thermoplastic polyurethane and polytetrafluoroethylene powder composites. Taylor & Francis. Vol.46 (2007), p. 575-578.

46. Bellingen C. V., N.P., Grivei E. - Journal of Vinyl & Additive Technology. (2006), p. 14-18.

47. Frogley M.D., Ravich D., Wagner H. D. - Composites Science and Technology. Vol. 63 (2003), p. 1647–1654.

48. Walder J., Whelihan M., Russell T., Rich A.- SAE paper 05M-497. 2004.

CHAPTER 2

LITERATURE REVIEW

Most important preparation methods of polymer composites are reviewed. A basic understanding of the different blending processes and available equipments are mentioned. The selected method is described in detail as well as its usage in dealing with polymer composites. Some fundamentals on morphological aspects and properties of thermoplastic elastomers are provided. Special attention is placed on thermoplastic polyurethane and styrene-butadiene-styrene composites. In order to have control on the level of dispersion of the micro- and nanofillers in a polymer matrix, we need to know the nature of such particles in terms of structure, morphology, texture, and chemistry. In this Chapter, we concentrate on the basic aspects of micro- and nanofillers, namely crude and exfoliated vermiculite, carbon nanofibers, high structure carbon black, nanoclay, nanosilica. A state-of-the-art of type of fillers used and their effects on the TPE properties is presented.

2.1. PROCESSING OF TPE BASED COMPOSITES

The need of reinforcing TPE with micro - and nanosize particles requires appropriate facilities for mixing, for controlling de-agglomeration and dispersion of fillers in polymers matrix. This new reinforcing materials are available in low quantities (few grams) because they are expensive to purchase at such early stages of development. Mixing is an extremely complex process because it can involve different basic operations, such as dispersing particles, wetting solid particles by the matrix, plasticizing, and uniformly distributing the particles to obtain a homogeneous compound.[1] To disperse nanoreinforcements, melt mixing methods are usually preferred due to the versatility of the production facilities. [2] Melt blending involves time and temperature-dependent non-Newtonian materials, and in addition, the flow field is a combination of shear and extensional flow.[3] During the blending process, melting and mixing are the most important and basic processing steps because melting affects the process rate, and mixing determines the morphology [4] In order to incorporate these materials into a new polymer material system, laboratory-scale mixing devices are essential. It is necessary for the mixer to be small enough to deal with tiny amounts of material, yet sufficiently powerful and appropriately designed to exert the shear stress and have the flow patterns essential for obtaining well-dispersed and uniform structures as in an industrial scale equipment [5], with minimize material waste.

There are several miniature mixers commercially available, such as twin-screw extruders, MiniMax™, recirculating screw mixer and internal batch mixers for polymer blends compounding of small grams of material in the range of 1-10 g. However, the final blend morphology in these mixers is coarse, with many large dispersed phase domains existing even after 20 minutes of mixing time. [5] Our goal is to compound polymer blends in small quantities so that we can predict the morphology expected in larger production scale, without consuming large quantities of polymer. therefore it was required a better dispersive mixer.

Sundararaj et all have developed a mini mixer called Alberta Polymer Asymmetric Minimixer (APAM). [5] This mixer has a unique, asymmetric design consisting of a varying clearance between the rotor blade tips and the cup wall, enabling the material to be squeezed, stretched and kneaded in high shear and converging zones. [5,6] Unlike the few other miniature mixing devices that are commercially available, the APAM has a combination of good mixing capability and complex flow modes required for dispersive flow, and requires minimal sample mass.[5] Small enough to deal with tiny amounts of material, yet sufficiently powerful and appropriately designed to exert the shear stress and have the flow patterns essential for obtaining well-dispersed and uniform structures as in industrial scale equipment [5], while

minimizing material waste. In a study made by Sundararaj et all comparing the blending results of APAM with the mixers above mentioned, there was evident the superior results of APAM, showing a well-dispersed structure.[3,5,6] For this work a miniature mixer was developed based on APAM.

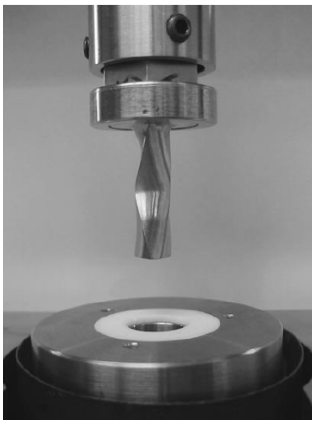

Figure 2.1 - APAM.[5]

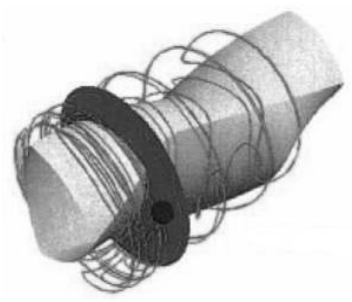

Figure 2.2 - Particle tracking and path in the metal cup.[6]

2.2.THERMOPLASTIC ELASTOMER

2.2.1.Thermoplastic polyurethane, TPU

Thermoplastic polyurethane elastomers, belong to the class of TPE that combine the mechanical properties of vulcanized rubber with the processability of thermoplastic polymers. They can be repeatedly melted and processed due to the absence of the chemical networks that normally exist in rubber. TPU are linear segmented block copolymers having hard segments (HS) and soft segments (SS).[7] TPU are based on the exothermic reaction of polyisocyanates with polyol molecules, containing hydroxyl groups. Relatively few basic isocyanates and a range of polyols of different molecular weights and functionalities are used to produce the whole spectrum of polyurethane materials. Two types of diisocyanates are employed in polyurethane preparations, aromatic and aliphatic ones. Most commonly used chemical structures are the aromatic diisocyanates; toluene diisocyanate (TDI), and 4,4'-diphenylmethane diisocyanate (MDI) (Figure 2.3). [7] TPU are usually made from pure MDI which is reacted with a substantially linear polyether or polyester diol [7,8] and with a chain-extending diol of a low molecular weight, such as 1,4-butanediol, (BDO) in either a one-step or a two-step reaction process. [86] The polyester diols are usually the condensation products of adipic acid and one or more simple aliphatic diols ranging from ethylene glycol to 1,6- hexanediol.

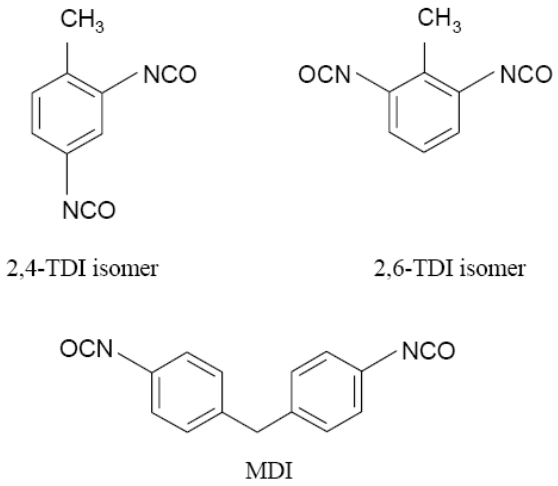

Figure 2.3 - Molecular structures of most common industrial isocyanates.

The HS act as crosslinks, inhibiting stress-relaxation and inducing stress-crystallization, which results in higher tensile strength. [9] The SS form an elastomer matrix which accounts for the elastic properties of TPU. [7] At room temperature, the low melting SS are incompatible with the polar high melting HS, which leads to a microphase separation and, consequently, to a polydomain structure. [7]

The HS segregates into a glassy or semicrystalline domain, and the polyol SS form an amorphous or rubbery matrix in which the HS are dispersed. [10,11]With the increase on the level of rigid segments, the TPU generally shows an increment on hardness, accompanied by a higher glass transition temperature. The ratio of thermoplastic or rubber phases determines the nature and properties of the product. The tendency to crystallize of the flexible segments is observed during the low and medium stretching, and this result in an induced crystallization affecting the modulus and strength.

TPU are used in applications where a product requires excellent tear strength, abrasion resistance & flexual fatigue resistance, chemical/oil resistance, low permeability to oils and fuels, resistant to radiation exposure. Mechanical properties of the polyester TPU are generally higher. Additives can improve dimensional stability, heat resistance, reduce friction, or increase flame retardancy or weatherability. Service temperatures range from - 50 °C to 150 °C and all have excellent adhesion properties. These materials have generally offer better strength and rigidity properties than conventional thermoset rubbers and their high elasticity confers exceptional dynamic flex properties.

2.2.2.Poly(styrene–butadiene–styrene), SBS

Poly(styrene–butadiene–styrene) rubber, was developed at the beginning of the 1960s. [12-14] A tri-block copolymer, SBS belongs to the group of thermoplastic elastomers made by anionic polymerisation. [15] This material consist of two phase structures, a rigid polystyrene segments giving its durability and soft butadiene segments giving SBS its rubber-like properties. [16,17] Polybutadiene glass transition temperature is around -80°C and polystyrene around 90°C.

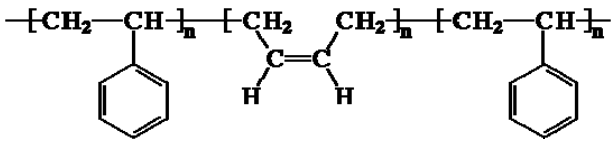

Figure 2.4 - Chemical structure Styrene-Butadiene-Styrene.

Unlike the repeat unit in a statistical copolymer, the repeat units in a block copolymer are arranged in separate blocks. In SBS rubber, each polymer chain consists of three sections, two outer sections made from styrene monomers and a middle section made from butadiene monomers. Since the different chain blocks are actually immiscible in one another, the styrene blocks phase separate from the butadiene blocks. [18]

SBS behave like elastomeric rubbers at room temperature but when heated can be processed like plastics. Most types of rubber are difficult to process because they are crosslinked. But SBS manage to be rubbery without being crosslinked, making them easy to process into nifty useful shapes. [17] This means it can be heated and re-mold unlike covalently crosslinked elastomers. [18]

With low polystyrene content, the material is elastomeric with the properties of polybutadiene predominating. This gives the material the ability to retain its shape after being stretched. [17,19] SBS exhibit good resistant to low temperature, good permeability, elongation percentage, and outstanding elasticity. [12,13] Commonly used in footwear, adhesives and tire treads food and cosmetics packaging.

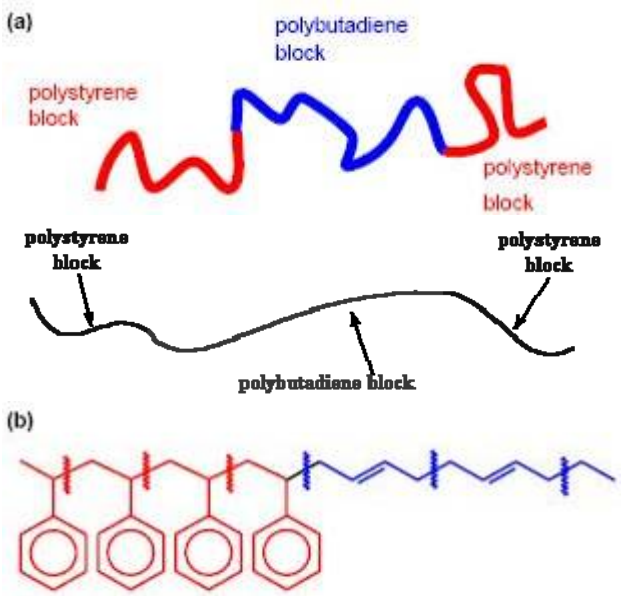

Figure 2.5 - (a) Very simple schematic view of the SBS block copolymer molecule. (b) Chemical structure of the polystyrene and polybutadiene sections. Parts formed from styrene monomers (red) and butadiene monomers (blue) are marked. [15]

2.3. MICROPARTICLES

Vermiculite VC, belongs to the phyllosilicate group of minerals, the mineralogical name given to hydrated laminar magnesium aluminum-iron silicate which resembles mica in appearance [20,21]VC is a 2:1 clay, meaning its crystal lattice consists of one octahedral sheet sandwiched between two opposing tetrahedral sheets. [21] A tetrahedral sheet is composed of corner-linked tetrahedra, whose central ions are Si^{4+} or Al^{3+}.[21] The octahedral sheet is composed of edge-shared octahedra with Mg^{2+}, Al^{3+}, or Fe^{2+}. Due to isomorphic substitutions which are Al^{3+} for Si^{4+}substitution in tetrahedral layers and Mg^{2+} or Fe^{2+} for Al^{3+} substitution in octahedral layers, VC layers have permanent negative charges. [21] VC is found in various parts of the world, and is recognized for their excellent intercalation abilities. [22] It is formed by hydration of certain basaltic minerals, and is often found in association with asbestos. T is a safe and inert mineral, characteristically yellowish brown in color. When heated it expands (exfoliates) up to 30 times it original volume. Natural and non toxic mineral that expands with the application of heat, are microsize particles between 0.1 and 100 μm in size. The expansion process is called exfoliation.

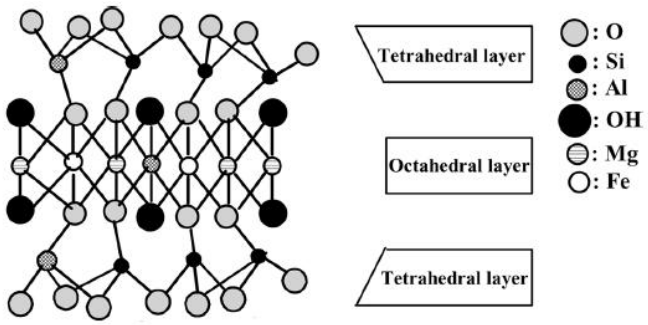

Figure 2.6 – Structure of vermiculite- Its chemical composition: $22MgO.5Al_2O_3.Fe_2O_3.22SiO_2.40H_2O$. [21]

VC has a medium shrink-swell capacity and is considered a limited-expansion clay. When VC is subjected to fast heating, its interlayer crystalline water transforms into steam and the pressure of steam forces the silicate layers apart from one another in which the K^+ ions between the molecular sheets are replaced by Mg^{2+} and Fe^{2+} cations. As a result, expanded VC with a large pore volume, light and clear, a low bulk of density, and a high heat isolator and sound-proof property; [23] refractory insulation material is obtained. easily handled, odorless, and low-cost material.VC has been used in various industries for over 80 years: construction, agricultural (as fertilizer carrier, adsorbent, etc.), horticultural, and industrial markets(as fire protection, acoustic and thermal insulator, additive in concrete and plaster, packaging material, etc.), and environmental (as adsorbent) applications. [21,24] The bulk density of crude vermiculite (VCC) is in the range of 640-1120 kg/m^3 and exfoliated or expanded vermiculite (VCE) is in the range of 64-160 kg/m^3. [20]

2.4. NANOPARTICLES

Nanoparticles are ultrafine particles with nanometer dimensions, about 1 to 100 nm, [25] showing size dependency of the properties of composites. [26] There are different types of nanoparticles made out from very wide variety of materials, regarding their origin commercially availability, dimension and geometry. Normally, microparticle additives require much higher loading levels to achieve similar performance than nanoparticles with low loading levels. This can result in significant weight reductions, coming in wide interest and importance for military and aerospace applications. The nanoparticles can be incorporated in a polymer matrix either during polymerization or by melt compounding forming polymer nanocomposites, depending on the application.

2.4.1.Platelet Shape

2.4.1.1.Montmorillonite, MMT

The significant feature of layered silicates, in comparison to other more commonly used, is their high aspect ratio and their ability to be readily dispersible on a nanometer scale. [27] The essential nanoclay (NC) raw material is MMT a 2-to-1 layered smectite clay mineral with a platelet structure. Individual platelet thicknesses are just one nanometer, but surface dimensions are generally 300 to more than 600 nanometers. Naturally MMT is hydrophilic. Since polymers are generally organaphilic, unmodified NC disperses in polymers with great difficulty. Through clay surface modification, MMT can be made organophilic and, therefore, compatible with conventional organic polymers. [2,28,29] Natural clay, containing an inorganic cation in the interlayer, are hydrophilic. After cation exchange of an inorganic cation to a large organic cation, the clay properties are altered and the material becomes hydrophobic. [22] Surface compatibilization is also known as "intercalation". Compatibilized NCs disperses readily in polymers. When NCs are dispersed and exfoliated in a polymer matrix, they form a near-molecular blend called a nanocomposite. [30]

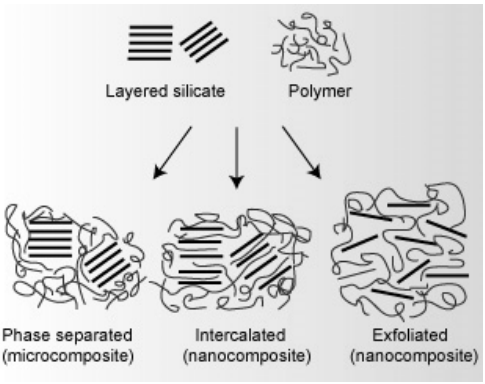

Figure 2.7 – Nanoclays dispersion in a polymer matrix.

This special structure of the layers results in an unusually high aspect ratio that makes NCs superior to all other conventional layered fillers. [29] These minerals considerably increase the mechanical and thermal properties of polymers through improving fire resistance by formation of a three-dimensional network, smoke emissions, chemical resistance, surface appearance, improved transparency, electrical conductivity, and barrier properties [31] usually resulting from the synergistic effect between organic and inorganic components. [8] This improvement of the properties may be reached with a very low concentration of NC. [29] The density of the NC reinforced polymers does not suffer significative changes leading to a definite weight advantage especially in the area of automotive applications. [29]

The properties of NCs strongly depend on the organic matrix, the nanoparticle, and the way in which they are prepared. [8] [1] The best properties are achieved if the clay is fully exfoliated. Their small size also results in small inter-platelet distances in a polymer/clay nanocomposite. [31]

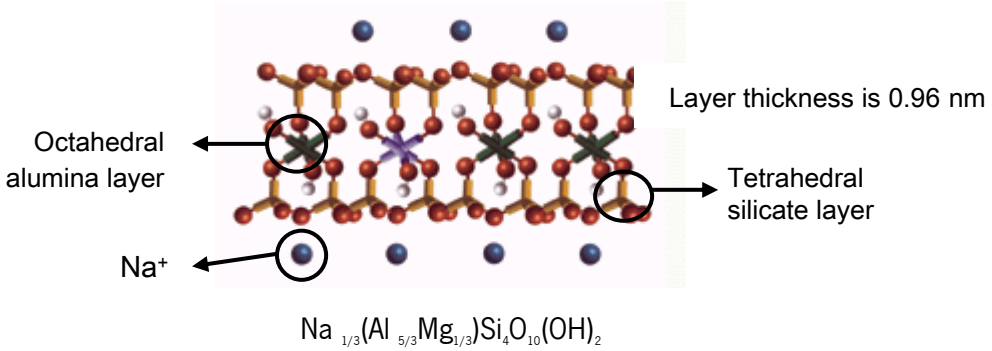

Figure 2.8 - Chemical structure of montmorillonite nanoclays.

In the scope of this work, the platelet-like shape nanoparticles of organo-modified layered silicates, MMT, namely, Nanofil 5 (distearyl-dimethyl-ammonium ion exchanged bentonite, recommended for polyesther based polymers) are supplied by Süd-Chemie AG, Germany. This NC have long chain hydrocarbon, as it is schematically presented in the following.

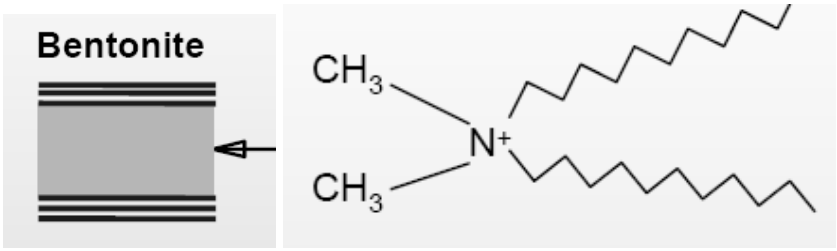

Figure 2.9 - Chemical functionalization of nanoclays (Nanofil 5).

2.4.2.Spherical Shape

2.4.2.1.Nanosilica, SiO_2

Nanosilica (NS) consists on spherical particles having a diameter less than 100 nm. Chemically speaking, they are made of silicon and oxygen atoms. Because their surface properties, particle size and their tendency to aggregate in the organic matrix on account of their high surface energy, it is very difficult to predict the properties of newly prepared nanocomposites.

Although silica was up to now widely used in polymer formulation as additives to master the system rheology and enhance mechanical properties of some particular polymers, NS throws the door wide

open for new applications. Silica synthesis evolved during last decades from thermal hydrolysis of silane resulting in not easily dispersible aggregated nanoparticles to sol-gel process resulting in well-defined nanoparticles, highly compatible with the targeted matrix. Processes enabling chemically tuned and well integrated particles together with the nanoscale effect are a highway to high performance nanocomposite materials having enhanced mechanical properties and excellent surface properties. [32]

2.4.2.2.High Structure Carbon Black, HSCB

Carbon black is an amorphous form of carbon with a structure similar to disordered graphite [33] that has a high surface area-to-volume ratio produced by incomplete combustion or thermal decomposition of gaseous or liquid hydrocarbons under controlled conditions. [34] [2] When aromatic hydrocarbons are placed to incomplete combustion of carbon-containing materials, such as oil, fuel oils or gasoline, natural gases, coal, paper, rubber, plastics and waste material at high temperature, their molecules will dissociate through the rupture of C-H bonds. Also contain large quantities of dichloromethane- and toluene extractable materials, and can exhibit an ash content of 50% or more. [34]

Smaller particles have higher inter-aggregate attractive forces (Van der Waals forces), resulting into a high secondary structure and an increased agglomerate size. This also means that the dispersion process requires more energy to separate them. [35] If the aggregates are composed of few prime particles, carbon black is designated a low structure carbon black. A high structure carbon black consists of relatively many prime particles. Because high structure carbon blacks tend to produce larger aggregates, consequently higher electrical conductivity at the same loading of low structure carbon black can be shown. [36,37]

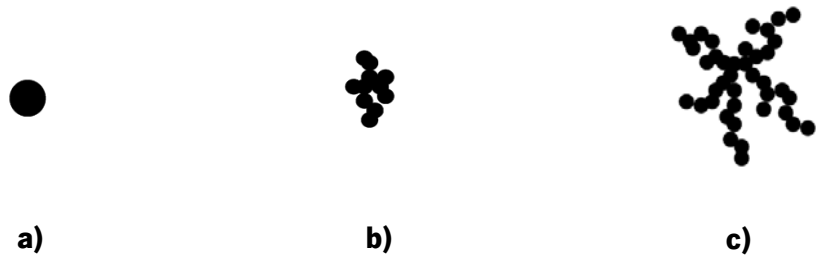

Figure 2.10 - a) Low structure (individual particles); b) Low structure (low agglomeration); c) High structure (with a high degree of openness and chaining)

Its use in tires, rubber and plastic products, is related to properties of specific surface area, particle size and structure, conductivity and color. Approximately 90% of carbon black is used in rubber applications, 9% as a pigment, and the remaining 1% as an essential ingredient in hundreds of diverse applications.

2.4.3.Carbon Nanofiber, CNF

Carbon has two well known crystalline forms (diamond and graphite) but it also exists in quasicrystalline and glassy states. As far as fibers technology is concerns *graphite* is the most important structural form of carbon. The graphite structure consist of hexagonal layers, in which the bonding is covalent and strong (~525kJ/mol); these layers, which are called the basal planes, and they are stacked in an ABAB— sequence, as shown in Figure 2.11, and have weak (<10kJ/mol) inter-layer bonds. The properties of graphite are very anisotropic. The theoretical elastic modulus of graphite is approximately 1000 GPa in the basal plane and only 35 GPa in the c-direction perpendicular to these planes. [38]

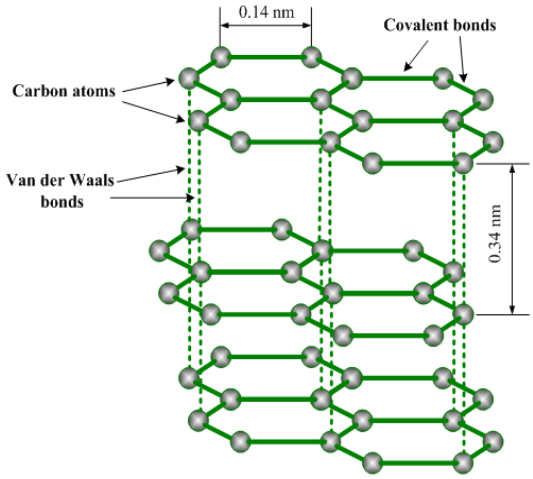

Figure 2.11- Crystal structure of graphite.

Graphite sublimes at 3700°C but starts to oxidize in air at around 500°C; carbon fibers can however be used at temperatures exceeding 2500°C if protected from oxygen. Carbon is a good electrical conductor. [38]

CNFs are an important class of graphite-related materials produced from the catalytic decomposition of hydrocarbon gases or carbon monoxide over selected metal particles that include iron, cobalt, nickel, and some of their alloys at temperatures over the range 400±1000°C. This process is termed Catalytic Chemical Vapor Deposition. CNFs are composed of 90 % by weight of elemental carbon and the rest is made various elements mainly oxygen and hydrogen. Different types of defects are present on the surface such as vacancies, dislocations, edges and steps. [39] CNFs have extraordinary mechanical, electrical, and thermal properties and their combination with polymers offers properties improvement breeding a new composite material with promising scientific enhancement.

CNFs are mainly differentiated from nanotubes by the orientation of the graphene planes: whereas the graphitic layers are parallel to the axis in nanotubes, nanofibers can show a wide range of orientations

of the graphitic layers with respect to the fiber axis. CNF composites reaches percolation threshold at only a few volume or weight percents of CNFs, markedly lower than metal particles or carbon black due to high aspect ratio and nanoscale size allowing CNFs to form conductive networks much more efficiently, [40-42] suitable for electrical conductive components, antistatic, electrostatically dissipative, and electromagnetic shielding and sensor applications.

2.5. STATE-OF-THE-ART

It has been long since the first introduction of reinforced polymers into engineering practices, and they have found a prominence place among common materials. There use in various applications requires not only good mechanical properties as well as processing facilities. Their application in new areas, means that other properties must be developed to meet the desired functionality without affecting the polymer properties. In nanoparticles based polymer composites, physical bonding between filler and matrix is very critical for producing a high performance composite. [39] A prerequisite for a good polymer-nanofiller composite is to have an adequate interfacial adhesion between the inorganic and the organic material. The extent of interfacial contact depends on contact angle and viscosity behaviour of the nanocomposite. [39] The type of filler, their dispersion, their incorporation level, determines mechanical and thermal properties, and is fire behavior of the final composite system, as well as the electrical resistivity. [41,43-54]

In recent years, TPE nanocomposites, long have erne the interest of scientific community showing improved performance and leading to a number of changes in physical properties, due to incorporated fillers high surface area and significant aspect ratios. [55-57] In particular, TPEs have been filled with several nanoparticles, such as NC, NS, HSCB, CNF, in order to improve properties like heat resistance, mechanical properties, anti-static/electrical properties, etc. and the achievement of multifunctional behaviour.

Polymer nanocomposites can be prepared using different methods, including in-situ polymerization, solution processing and melt mixing [58,59] Melt mixing is the preferred method because it is environmentally benign and it is compatible with current industrial processes. [58-60] However, it is difficult to mix [61] homogeneously material such as nanoparticles into a polymer matrix due is natures and because of the existence of synthesis-induced entangled aggregates and the high van der Waals interactions between nanoparticles. [58-60,62]

In the last years, a huge research effort has been allocated to study the reinforced thermoplastics. [63,64] Researchers have found the useful advantage of using NC for TPEs properties enhancement. The first report on the use of NC with elastomeric polyurethane was from Wang and Pinnavaia in 1998. [65] These nanocomposites showed significant improvement in tensile strength and tensile modulus, although the clay particles remained mostly in intercalated states. Volker Altstadt et. al [66] showed improvement of the mechanical properties and creep resistance of SBS block copolymers also by NC incorporation. J. Shen at al. [67] have study TPU filled with MMT by melt blending and observed that NC can also improve TPU thermal stability. [67][3] Wang and Pinnavaia [65] compared TGA measurements of intercalated and exfoliated organically modified magadiite nanocomposites and observed that the exfoliated nanocomposite showed thermal improvements. Other studies have shown that the introduction of these particles reduces heat release and improve the fire retardancy. [68]

Same mechanical improvement was observed with the use of NS. Wei-Dian Shen et al. Study the properties of TPU/silica (5% to 20% of incorporation) and shown that the incorporation of a small amount of NS increased the hardness, abrasion resistance, and tensile properties of the polymers, but, these mechanical properties could be worsened at higher NS contents. [69] The increase loading percentage may reduce some of the properties TPE. There is a limit amount of incorporation without injuring their mechanical and thermal properties maintaining a desired processability. Similar results have been reposted by Gupta et al. [70] These limitations encourages researchers to further study the application of this reinforce particles on TPE. [71] But it is still needed to understand them better, according to the microstructure / morphology of the material.

No publications were found, by using with crude and exfoliated vermiculite (VCC and VCE).

Polymers characteristically have a very high electrical resistance. [71] When conductive grades are required, base polymers are modified to prevent unwanted accumulation of charge or a conductive pathway. A part of developed work conducted on carbon composites is motivated by the potential of these fillers in TPE properties improvement, making them attractive and of critical importance for the integration in a wide range of high performance applications, e.g., aerospace structural components, heat exchangers, heat sinks, [73,74] sensors and active electrodes. [75]
In the last few years some systematic studies of the thermo-physical [76] and electrical properties [77] of composites has been published. Carbon materials also have great potential to be economically important for thermal management as observed by Zhou et al.. [78] Carbon nanofillers like HSCB and CNF are excellent candidates for multi-functional nano-reinforcing for TPEs because of their high

strength, modulus, high thermal conductivity (higher than copper and silver suitable for thermal management applications), excellent electrical capacity, and thermal stability. Vaia et al [79,80] have evaluated CNFs as TPE reinforcing agents. They observed that low amounts of CNF (1 to 5% of incorporation) lead to TPU mechanical and electrical property improvements

The electrical properties of a composite are determines by the volume fraction of the conductive filler, structure properties, orientation in the matrix, porosity and mixing conditions as observed by Khastgir et al. [81-83] when a study SBS filled with carbon black electrical and mechanical behavior. Homer et al. [76] observed that electrical properties of a composite also depends on the physico-chemical properties of both polymer and filler, such as particle size, shape, porosity, surface area, e.g., smaller and spherical particles or fibers and longer particle affect differently, as well as the composite processing conditions, such as temperature, etc.

For a conductor-filled polymer to be electrically conductive, the filler particles must either touch to form conductive paths, [41] or be sufficiently close to each other to enable conductance via ‘‘tunneling effect’’ as observed by Sheng et al.. [84,85] This is usually defined as the percolation transition, characterised by a sharp drop in the electrical resistivity and the critical weight or volume fraction of filler is the threshold dividing the composite into insulator and conductor. [76]

2.6. REFERENCES

1. Nortey N.O. Int Polym Process. Vol.16 (2001), p. 87.
2. Aso O., Eguiazábal J.I., Nazábal J. - The influence of surface modification on the structure and properties of a nanosilica filled thermoplastic elastomer. Composites Science and Technology. Vol.67: nº 13 (2007), p. 2854-2863.
3. Lin B., Sundararaj U., Guegan P. - Effect of Mixing Protocol on Compatibilized Polymer Blend Morphology. Polymer Engineering and Science. Vol.46: nº5 (2006), p. 691-702.
4. Grulke E.A. - Polymer Processing Engineering, Prentice-Hall. New Jersey,1994.
5. Breuer O., Sundararaj U., Toogood R. W. - The Design and Performance of a New miniature mixer for specialty polymer blends and nanocomposites. Polymer Engineering and Science. Vol.44: nº5 (2004).
6. Breuer O., Chen H., Lin B., Sundararaj U. - Simulation and Visualization of flow in new miniature mixer for multiphase polymer systems,. Journal of applied polymer science. Vol.97 (2005), p.136-142.
7. Frick A., Rochman A. - Characterization of TPU elastomers by thermal analysis (DSC). Polymer Testing. Vol. 23: nº4 (2004), p. 413-417.
8. Ciobanu C., Constantin X.H., Cascaval N., Guo F., Rosu D., Ignat L., Moroi G. - Influence of urethane group on properties of crosslinked polyurethane elastomers. Journal of Applied Polymer Science. Vol.87: nº11 (2003), p. 1858-1867.
9. Wilkes C.E., Yusek C. S. - Investigation of domain structure in urethane elastomers by X-ray and thermal methods. Journal of Macromolecular Science and Physics. B7, (1973), p.157-175.
10. Oertel G. Polyurethane Handbook. 2nd ed. New York: Hanser,chapter 2, 1993 p. 7. .
11. Navarro-Bañón V., J.V.-B., Vázquez P., Martín-Martínez J. M. - Interactions in Nanosilica-Polyurethane Composites Evidenced by Plate-Plate Rheology and DMTA. Macromolecular Symposia. Vol. 221: nº1 (2005), p. 1-10.
12. Honeker C.C., Thomas E.L. - Impact of Morphological Orientation in Determining Mechanical Properties in Triblock Copolymer Systems. Chemistry of Materials. Vol.8: nº8 (1996), p. 1702-1714.
13. Chen Z., Gong K. - Preparation and dynamic mechanical properties of poly(styrene-<I>b</I>-butadiene)-modified clay nanocomposites. Journal of Applied Polymer Science. Vol. 84: nº8 (2002), p. 1499-1503.

14. Holden G, Leggen N.R., Quirk R.P., Schroeder H.E. (Eds). - Thermoplastic Elastomers, 2nd ed. Hanser: New York, 1996.
15. http://www.azonano.com/Details.asp?ArticleID=2076
16. www.distrupol.com
17. http://pslc.ws/macrogcss/sbs.html
18. http://membership.acs.org/C/Chicago/statefair/CD-2007/Chemmatters/2007_4_tg.pdf
19. www.wikipedia.org.
20. http://www.vermiculite.org/aboutvermiculite.htm
21. Duman O., Tunç S. - Electrokinetic Properties of Vermiculite and Expanded Vermiculite: Effects of pH, Clay Concentration and Mono- and Multivalent Electrolytes. Separation Science and Technology. Vol. 43: n°14 (2008), p. 3755 - 3776.
22. Martynková G. S.,Valášková M., Šupová M. - Organo-vermiculite structure ordering after PVAc introduction. Physica Status Solidi(a). Vol. 204: n°6 (2007), p. 1870-1875.
23. Gordeeva L.G., Moroz E.N., Rudina N.A., Aristov Y.I. - Formation of porous vermiculite structure in the course of swelling. Russ. Journal of Applied Chem. Vol. 75: n°357 (2002).
24. http://www.palabora.com.
25. http://www.chm.bris.ac.uk/webprojects2002/etan/Webpages/.
26. Gangopadhyay R., De, A. - Conducting Polymer Nanocomposites: A Brief Overview. Chem. Mater. Vol.12 (2000), p. 608.
27. Becker O., Simon G.P. - Epoxy layered silicate nanocomposite. ed. Springer. Advance Polymer Science. Berlin Heidelberg, Vol. 179 (2005).
28. Petrovi Z.S, Zavargo Z., Flyn J.H., Macknight W.J. - Thermal degradation of segmented polyurethanes. Journal of Applied Polymer Science. Vol.51: n°6 (1994), p. 1087-1095.
29. www.sud-chemie.com.
30. http://www.nanocor.com/nano_struct.asp.
31. Patil N.V. - Nanoclays make polymers stronger: polymer clay nanocomposites considerably increase the mechanical and thermal properties of polymers. Advanced Materials & Processes. December 1, 2005. p. 39-40.
32. http://becomeananoist.com/index.php?Nanosilica.
33. Jan-Chan, H., Carbon black filled conducting polymers and polymer blends. Advances in Polymer Technology. Vol. 21: n°4 (2002), p. 299-313.
34. http://carbon-black.org/what_is.html.

35. Medalia A.I. - Electrical Conduction in Carbon Black Composites. Rubber Chemistry Technology. Vol. 59 (1986), p. 432.

36. Carmona F. - Conducting filled polymers. Elsevier. Vo. 157: n° 1 (1989), p. 461-469.

37. Balberg I. - Tunneling and nonuniversal conductivity in composite materials. Physical Review Letters Vol. 59: n°12 (1987), p. 1305.

38. Matthews F.L., Rawlings R.D. - Composite materials: Engineering and science. Chapman &Hall, 1 st. Ed., 1994.

39. Ehrburger P., Vix-Guterl C. - Surface Properties of Carbons for Advanced Carbon-based Composites, In: Design and Control of Structure of Advanced Carbon Materials for Enhanced Performance, Yardim, M. F., Ed.; Kluwer Academic Publishers, Netherlands: Netherlands, 2001.

40. Celzard A., McRae E., Deleuze C., Dufort M., Furdin G., Marêché J. F. - Critical concentration in percolating systems containing a high-aspect-ratio filler. Physical Review B. Vol.53: n°10 (1996), p. 6209.

41. Vu Y.T., Mark J.E., Pham L.H., Engelhardt M. - Journal Applied Polymer Science. Vol. 82 (2001), p.1391 .

42. Sandler J., Shaffer M. S. P., Prasse T., Bauhofer W., Schulte K., Windle A. H. - Development of a dispersion process for carbon nanotubes in an epoxy matrix and the resulting electrical properties. Polymer Engineering and Science. Vol. 40 (1999), p. 5967-5971.

43. Kawasumi M., Hasegawa N., Kato M., Usuki A., Okada, A. Macromolecules. Vol. 30 (1997), p.6333.

44. Godgire P., Kalgaonkar R., Hambir S., Bulakh N., Jog J.P. Journal of Applied Polymer Science. Vol. 81 (2001), p.1786.

45. Whang M.Q., Rong M.Z., Zeng H.M., Schmitt S., Wetzel B., Friedrich K. Journal of Applied Polymer Science. Vol. 80 (2001), p. 2218.

46. Alexandre M., Debois P., Sun T., Garces J.M., Jérôme R. Polymer. Vol. 43 (2002),p. 2123.

47. Ma J., Zhang S., Qi Z., Journal of Applied Polymer Science. Vol. 82 (2001), p.1444.

48. Sadhu, S., Bhowmick A.K, Journal of Applied Polymer Science. Vol.92 (2004), p. 698.

49. Sadhu, S., Bhowmick A.K. Journal Polymer Science: Polymer Physics. Vol. 42 (2004), p.1573.

50. Sadhu, S., Bhowmick A.K. Rubber Chemistry Technology. Vol.76 (2003), p. 0860.

51. Donnet J.B., Bansal R.C., Wang M.J. - Carbon Black—Science and Technology, 2nd Ed. Marcel Dekker: New York, 1993.

52. Dresselhaus M.S., Dresselhaus G., Eklund P.C. - Science of Fullerenes and Carbon Nanotubes. Academic Press, 1996.

53. Iijima S. Nature. Vol. 56 (1991) p. 354.

54. Strumpler R., Glatz-Reichenbach J. - Conducting Polymer Composites, J. Electroceramics. Vol.3: n°4 (1999), p.329-346.

55. Becker O., Simon G.P. - Epoxy Layered Silicate Nanocomposites. Advances in polymer science. Vol. 179 (2005), p. 226 (0065-3195).

56. Holister P., Weener J.W., Vas C. R., Harper T. Nanoparticles Cientifica. Technology White papers. n°3, 2003.

57. Becker O., Simon G.P. - Epoxy Layered Silicate Nanocomposites. Advances in polymer science. Vol. 179 (2005), p. 226 (0065-3195).

58. Breuer O., Sundararaj U. Polymer Composites. Vol.25 (2004), p.630.

59. Lin B., Sundararaj U., Guegan P. - Effect of mixing protocol on compatibilized polymer blend morphology. Polymer Engineering & Science.Vol. 46: n°5 (2006), p. 691-702.

60. Ray S.S., Okamoto M. Prog. Polymer Science. Vol. 28 (2003), p.1539.

61. Siriwardena S., Ismail H., Ishiaku U. S., Perera M. C. S. Journal of Applied Polymer Science. Vol. 85 (2002), p.438–453.

62. Potschke P., Bhattacharyya A. R., Janke A., Goering H. Compos. Interfaces. Vol. 10 (2003), p.389.

63. Pal P.K., De S.K. Rubber Chemistry and Technology. Vol. 56 (1983), p. 737.

64. Rozman H.D., Peng G.B., Ishak Z.A.M. Journal of Applied Polymer Science. Vol.70 (1998), p.2647.

65. Wang Z., Pinnavaia T.J. Chem. Mater., Vol.10 (1998), p.769.

66. Lietz S., Yang J-L., Bosch E., Sandler J.K.W., Zhang Z., Altstädt V.- Improvement of the Mechanical Properties and Creep Resistance of SBS Block Copolymers by Nanoclay Fillers. Macromolecular Materials and Engineering. Vol. 292: n°1 (2007), p. 23-32.

67. Zou H., Ran Q., Wu S., Shen J. Polymer Composites. 2008,p. 1-5.

68. Wang Z-Y., Han E.-H., Kei W. - Fire-resistant effect of nanoclay on intumescent nanocomposite coatings. Journal of Applied Polymer Science. Vol.103: n°3 (2007), p. 1681-1689.

69. Zhou S-X., Wu L.-M., Sun J., Shen W-D. - Effect of nanosilica on the properties of polyester-based polyurethane. Journal of Applied Polymer Science. Vol. 88: n°1 (2003), p. 189-193.

70. Gupta A.K., Srinivasan K.R., Kumar K.P. Journal of Applied Polymer Science. Vol.43 (1991), p.451.

71. Knite M., Teteris V., Aulika I., Kabelka H., Fuith A. Advance. Engineering Material. Vol. 6: n°9(2004), p. 746-749.

72. BLYTHE A.R. - Electrical resistivity measurements of polymer materials. Polymer testing. Vol. 4: n°2-4 (1984), p. 195-209.

73. Biercuk M.J., Llaguno M.C., Radosavljevic M., Hyun J.K., Johnson A.T., Fischer J.E. -Carbon nanotube composites for thermal management. Applied Physics Letters. Vol. 80 (2002), p. 2767.

74. Benedict L.X., Vincent C.H., Steven L.G., Marvin C.L. - Static conductivity and superconductivity of carbon nanotubes: Relations between tubes and sheets. Physical Review B, Vol. 52: n° 20 (1995), p. 14935.

75. Gutiérrez M. P., Li H., Patton J. - Thin Film Surface Resistivity. Materials Engineering, Proc. Inst. Radio Engrs. Vol. 42 (2002), p. 420.

76. Homer M.L., Lim, J.R., Manatt, K., Kisor A., Manfreda, A.M., Lara L., Jewell A.D., Yen S.P.S., Zhou H., Shevade A.V., Ryan M.A.- Temperature effects on polymer-carbon composite sensors: Evaluating the role of polymer molecular weight and carbon loading in Sensors. Proceedings of IEEE. 2003.

77. Holliday L., Kelly A., F.R.S., Polymer engineering composites. Applied Science Publishers Ltd. 1977, London.

78. Zhou Y., Jeelani S., Eranezhuth B. - Improvement in thermal, mechanical and electric properties of multi-wall carbon nanotube reinforced epoxy and carbon/epoxy composite. eXPRESS Polymer Letters. Vol.2 (2008), p. 40–48.

79. Powers D.S., Vaia, R.A., Koerner H., Serres J., Mirau P.A. - NMR Characterization of Low Hard Segment Thermoplastic Polyurethane/Carbon Nanofiber Composites. Macromolecules. Vol. 41: n°12 (2008), p. 4290-4295.

80. Lai S.-M., Wang C.K., Shen H. F. - Properties and preparation of thermoplastic polyurethane/silica hybrid using sol-gel process. Journal of Applied Polymer Science. Vol. 97: n°3 (2005), p. 1316-1325.

81. Sau K.P., Chaki T.K., Khastgir D. - The change in conductivity of a rubber-carbon black composite subjected to different modes of pre-strain. Composites Part A: Applied Science and Manufacturing. Vol. 29: n°4 (1998), p. 363-370.

82. Leyva M.E., Barra G.M.O., Moreira A.C.F., Soares B.G., Khastgir D. - Electric, dielectric, and dynamic mechanical behavior of carbon black/styrene-butadiene-styrene composites. Journal of Polymer Science Part B: Polymer Physics. Vol.41: n°23 (2003), p. 2983-2997.

83. Mohanraj G.T., Chaki T. K., Chakraborty A., Khastgir D. - Effect of some service conditions on the electrical resistivity of conductive styrene-butadiene rubber-carbon black composites. Journal of Applied Polymer Science, 2004. 92(4): p. 2179-2188.

84. Simmons GJ. - Generalized formula for electric tunnel effect between similar electrodes separated by a thin insulating film. Journal of Applied Physics. Vol. 34 (1963), p. 1793–803.

85. Sheng P., Sichel E.K., Gittleman JL. - Fluctuation-induced tunneling conduction in carbonpolyvinylchloride composites. Physics Review Letters. Vol.40, 1978.

86. Randall D., Lee S., Woods G. - The polyurethanes book. Distributed by J. Wiley: New York, 2002.

CHAPTER 3

MOTIVATION AND OBJECTIVES

The motivation, main objectives of this research work, as well as the specific tasks are presented. At the end of the chapter a flow chart illustrates the experimental sequence used in this thesis.

3.1. MOTIVATION

The information provided in the preceding chapters has demonstrated that many investigations have confirmed the improved properties resulting from the addition of micro- and nanosized particles in many conventional thermoplastics and elastomers. From among the numerous advantages offered by micro- and nano-reinforcement, the possibility of achieving multifunction and enhanced properties needs to be still explored. With the addition of reinforcing particles, TPEs allow an adjustment of their properties, making them a versatile class of materials more advantageous compared to the thermoplastics and elastomers. Few studies have focus exclusively on exploring the use of micro- and nanoparticles particles for TPE properties and performance reinforcement. It is well known that nanocomposites require low amounts of nanofillers, but most of the publications on reinforced TPE have focus on the use of higher incorporation amounts (superior to 1%wt.[1-6]). Large volume fractions has demonstrated a negative impact in deformability, processibility, surface finish, and limit the ability to maintain desired conductivity at extreme deformations (>100%).

Faced with a growing interest of these composites it is important to study a new class of polymers composites, as a means to further reduce the incorporation percentage, and therefore the material cost.

3.2. OBJECTIVE

Driven by the importance of materials reinforcement (Chapter 1) and based on the research work embodied in this thesis, it is intended to provide a deeper knowledge in the:

-Validation of dispersion ability of the developed laboratory-scale miniature mixer;

-Evaluation of the incorporation effect of the different types of particles (eg. Micrometric and nanometric dimension) on multifunctional behavior, the mechanical, thermal and antistatic properties and TPEs (namely, TPU and SBS) flame behavior;

-Establish a relation between the developed morphology and the reinforced TPEs mechanical properties with different particles.

3.3. WORK PERFORMED

The materials selected for this research work, namely TPU and SBS, will be mixed with low amounts of microsize (crude and exfoliated VC) and nanosize (HSCB, CNF, NS, NC) particles through the following steps:

a) TPEs reinforcement preparation

- Setting the blending condition (temperature, rotation velocity, mixing time, incorporation %);
- TPE molded plates preparation;
- Evaluate the dispersion degree (Optical microscopy (OM), Scanning electron microscopy (SEM));
- Cut tensile test specimens for testing.

b) Morphological characterization

- TPEs functional groups identification (Fourier transform infrared spectroscopy);
- Evaluation of the agglomeration, dispersion and particles adhesion in the matrix through microscopic techniques (OM, SEM);
- Particles/aggregate dimension evaluation (OM, SEM);
- Analysis of the fractured surface and morphological characterization of the deformed material;

c) Properties characterization

- Composites Melt Flow Index measurement.
- Mechanical characterization (Tensile tests, hardness);
- Thermal characterization (Thermagravimetric analysis, Scanning electron microscopy, thermal conductivity);
- Flame behavior characterization (flame tests);
- Electrical characterization (electrical resistivity);

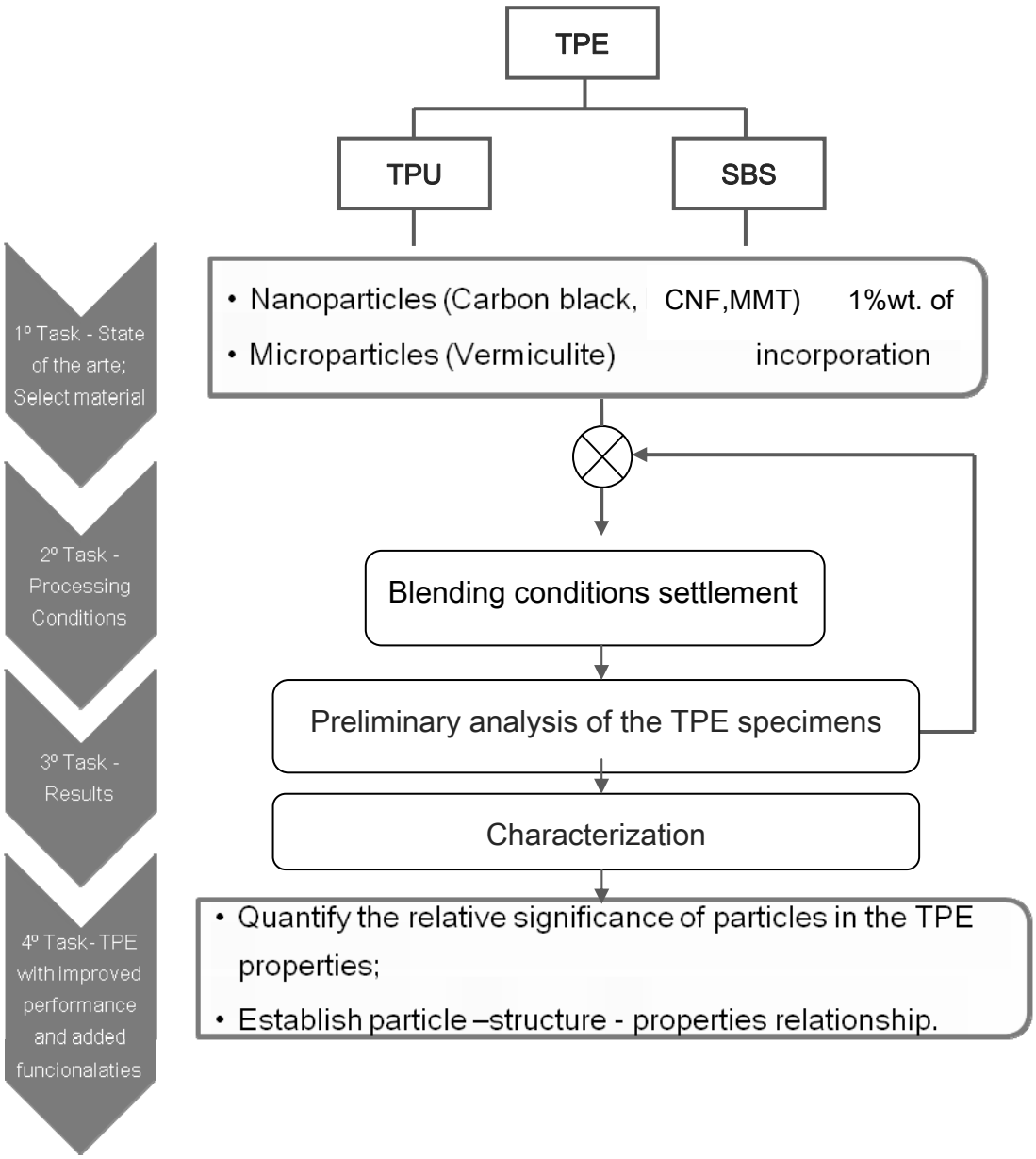

Figure 3.1 - Experimental sequence.

3.4. REFERENCES

1. Bellingen C.V., Grivei N.P.E. - Meeting application requirements with conductive carbon black. Journal of Vinyl and Additive Technology.Vol. 12: n°1 (2006), p. 14-18.
2. Homer M.L., Lim, J.R., Manatt, K., Kisor A., Manfreda, A.M., Lara L., Jewell A.D., Yen S.P.S., Zhou H., Shevade A.V., Ryan M.A.- Temperature effects on polymer-carbon composite sensors: Evaluating the role of polymer molecular weight and carbon loading in Sensors. Proceedings of IEEE. 2003.
3. Santos M. A., Mattoso L.H.C., Defácio R., Avlyanov J. - Compósitos de Borracha Natural com Compostos Condutivos à Base de Negro de Fumo e Polímero Condutor Polímeros: Ciência e Tecnologia. Vol. 11: n° 3 (2001); p. 126-134.
4. Koerner H., Liua W., Alexanderb M., Miraub P., Dowtyb H., Vaia R.A. - Deformation-morphology correlations in electrically conductive carbon nanotube–thermoplastic polyurethane nanocomposites. Polymer. Vol. 46: n°12 (2005), p.4405-4420.
5. Zou H., Wu S., Shen J. - Polymer/Silica Nanocomposites: Preparation, Characterization, Properties, and Applications, in American Chemical Reviews. Published on Web 08/23/2008.
6. Lai S.-M., Wang C.K., Shen H.F. - Properties and preparation of thermoplastic polyurethane/silica hybrid using sol-gel process. Journal of Applied Polymer Science. Vol. 97: n°3 (2005), p. 1316-1325.

CHAPTER 4

MATERIALS, EQUIPMENTS AND EXPERIMENTAL METHODS

This chapter provides information on the grades of the selected polymeric materials; micro- and nanoparticles characteristics; the experimental techniques and characterization methods.

4.1. MATERIALS

The experimental work was conducted using a thermoplastic polyurethane (TPU) and a styrene-butadiene-styrene (SBS). Micro- and nanoparticles were mixed with those polymers to assess the degree of dispersion and its effects on the mechanical, thermal and electrical properties.

4.1.1. Polymers

The TPEs used in this work were commercially available in the form of pellets. A thermoplastic polyurethane, TPU, amorphous-semicrystalline polyester based, AVALON 65 AE form Huntsman (Belgium) and one styrene-butadiene-styrene (SBS), Goldenplast (Italy). Table 4.1 resumes the principal properties of both polymers.

Table 4.1 – Physical and mechanical properties of the selected TPEs.

Property	TPU	SBS
Density, g/cm^3	1.18	0.932
MFI, g/10 min	21.30(200°C- 2.16Kg)	30 (190°C- 5kg)
Tensile strength, MPa	20	6.1
Melting temperature, T_m,°C	200	190
Hardness , Shore A	65	55

4.1.2. Reinforcing particles

AEROSIL 200 is a highly dispersed, hydrophilic fumed silica that is produced by high-temperature hydrolysis of silicon tetrachloride in an oxyhydrogen gas flame. The primary particles are spherical and free of pores. AEROSIL 200 consists entirely of amorphous silicon dioxide. It starts to sinter and turn into glass above 1200°C. Crystallization only occurs after heat treatment. One gram of AEROSIL 200 contains approximately 1 mol of silanol groups.[1]

Table 4.2 lists main properties of AEROSIL 200.

Table 4.2– Silica nanoparticles detail technical specification.[1]

Name	Average primary particle size[nm]	Specific surface area[m^2g^{-1}]	Tapped density [gl^{-1}]	Behaviour toward water
AEROSIL 200	12	200 ± 25	≈ 50	Hydrophilic

Nanofil 5 (distearyl-dimethyl-ammonium ion exchanged bentonite), supplied by Süd-Chemie AG, Germany is an organic modified nanodispersed layered silicate in form of powder. Primary particle size after complete dispersion is 100-500 nm x 1 nm. [2] Table 4.3 lists main properties of Nanofil 5.

Table 4.3 – Clay nanoparticles detail technical specification. [2]

Name	Medium particles size [nm]	Platelet thickness [nm]	Bulk density [gl^{-1}]	Specific weight [$g.cm^{-3}$]	Intercalation
Nanofil 5	8000	1	150	≈ 1.8	Distearyldimethyl-ammonium chloride

PRINTEX® XE 2 is a high structure carbon black with extraordinary properties. The major physical properties regarding conductive characteristics of carbon black - such as specific surface area, structure and pore volume - are entirely different from conventional carbon blacks. It imparts to rubber compounds excellent electrical conductivity. [3] Table 4.4 list main properties of PRINTEX® XE2.

Table 4.4 – High structure carbon black nanoparticles detail technical specification. [3]

Name	Medium particles size [nm]	Surface area [m^2g^{-1}]	Pour density [$g.dm^{-3}$]
PRINTEX® XE 2	30	910	130

Electrovac is as polymer-based, dust-free nanofiber masterbatches with 20 % carbon nanofofibers.[4] Table 4.5 resumes main properties of Carbon nanofibers.

Table 4.5 - TPU with carbon nanofibers detail technical specification. [4]

Name	Average diameter [nm]	Specific surface area [m^2g^{-1}]	Specific weight [$g.cm^{-3}$]	Young's modulus
Electrovac	80 - 150	20 – 100	≈ 1.8 - 2.1	≈ 500GPa

Hoben International Ltd., vermiculite L835D Micron is micronized, followed by exfoliation to give a product with a carefully controlled size distribution and a melting point of 1330 °C. [5] Palabora Europe Ltd., vermiculite (PMC PP&V Micron) is a crude vermiculite consisting of golden/brown flakes, un-expanded. [6] Table 4.6 list main properties of vermiculite based particles.

Table 4.6 - Vermiculite detail technical specification. [5,6]

Name	Particles size [μm]	Loose Bulk density [gl^{-1}]	Specific surface area[m^2g^{-1}]
Hoben	10 – 65	120	9.9
Palabora	710 – 250	700 – 1050	6.4

4.2. PROCESSING EQUIPMENT

The TPE composites were prepared by melt blending. For the proper blending process a laboratory-scale miniature mixer was developed based on existing prototype. [7] It aims at controling de-agglomeration and dispersion of fillers in polymers matrix.

Figure 4.1 - Design scheme of miniature mixer device.

Figure 4.2 - Cylindrical rotor.

4.3. EXPERIMENTAL METHOD

4.3.1. Composites preparation procedures

A list of composites systems that were prepared is shown in Table 4.7. First task on this stage of work was the settlement of the blending conditions (temperature, rotation velocity, blending time, incorporation %). Once settled, the same conditions were fixed and used for all mixtures.

Table 4.7 - Reinforcement and specimens.

Reinforcing fillers	Trade name/Producer	Specimens
Nanosilica	Aerosil 200: Degussa advance Nanomaterials(Germany)	TPU+NS SBS+NS
Nanoclay	Nanofil: SuD-Chemie AG	TPU+NC SBS+NC
High-structure Carbon Black	Printex XE 2-B:Degussa	TPU+HSCB SBS+HSCB
Carbon nanofibers	EMB11SG20 - TPU01,20%wt. CNF - TPU: Electrovac AG(Austria)	TPU+CNF
Nanoclay	Nanofil: SuD-Chemie	TPU+NC SBS+NC
Vermiculite	Hoben International Ltd. (UK) (micronized following exfoliation)	TPU+VCE SBS+VCE
	Palabora Europe Ltd. (UK) (Crude vermiculite, un-expande)	TPU+VCC SBS+VCC

In this work, TPE composites were compounded using a total of 20 grams of TPEs per sample and 1%wt. of reinforcement fillers. The TPEs were previously grinded into powder particles and dried (TPU at 100°C for 1-2 H and SBS at 60°C for 2-4 H). Materials were inserted on the heated metal cup of the miniature mixing device (Figure 4.1). After the polymer is melted, the cylindrical rotor (Figure 4.2) descends into the cup, pushing molten material into the cavity and then rotates at 220 rpm for 3min.

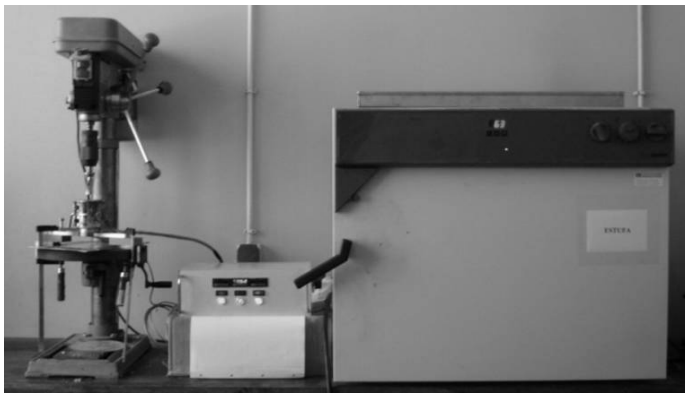

Figure 4.3 - Miniature mixer, Temperature controller and Oven (from left to right).

4.3.2. Compression moulding procedure

After mixing, the TPE blend is discharged on a metallic mold spacer 145 x 106 x 0,7mm thick and sandwiched between two stainless steel plates covered with Teflon foil (to facilitate plates removal) at a pressure of 774 MPa for 5 min at 190°C. This time was selected to ensure that the plates would be free of air bubbles and with an uniform 0,7mm thickness. Afterwards, the plates were quenched in water at room temperature (23°C). Fifteen plates were obtained, where two are pure TPE (TPU and SBS) that will be used for comparison, and thirteen are composite systems specimens (Table 4.7). All specimens were kept in a controlled temperature room (23°C) for at least 3 weeks before performing any experimental tests.

4.4. MORPHOLOGICAL CHARACTERIZATION

A preliminary dispersion, dimension of the particles/aggregates evaluation (for blending method validation) was performed by Optical microscopy (OM). The dispersion, exfoliation and adhesion between TPE and the reinforcement fillers were evaluated by scanning electron microscopy (SEM).

4.4.1. Fourier transform infrared spectroscopy, FTIR

FTIR spectra were recorded from 4400 cm^{-1} to 400 cm^{-1} in a reflectance mode and a resolution of 4 cm^{-1} in a spectrum BX II Perkin Elmer v53.1 spectrometer in order to identify TPEs composition.

4.4.2. Optical microscopy, OM, and image analysis

For a first evaluation of the micro- and nanoparticles distribution on the TPE matrix, OM was performed using a Polarized Light microscope Olympus I with a digital Leica camera. The 15 μm specimens were sliced from the central part of the specimens longitudinally to the flow direction with a microtome (Leitz1401 with a glass knife) previously freeze with CO_2. Afterword specimens were immersed in Canada balsam resin (with the same reflection index of the glass) between two microscopic glasses slides.

4.4.3. Scanning electron microscopy, SEM

The nanocomposites morphology, the dispersion, agglomeration and adhesion between the micro - and nanoreinforced fillers and the TPEs was observed by a scanning electron microscope (Leica/Cambridge S360 electronic microscope Cambridge, UK), operating at 10kv - 15kv. In order to avoid electrostatic charging the fractured (in liquid nitrogen) surface specimens were previous gold coated (Sputter Coater SC502, Fisons Instruments, U.K.).

4.5. PROPERTIES CHARACTERIZATION

Effect of particles incorporation on flow index, the mechanical, the thermal, the electrical properties, and the flame behavior was evaluated through a set of experimental tests of the molded plates. Because of the limited amount of material, TGA, DSC analysis and thermal conductivity and electrical measurements, only one sample for each condition was tested.

4.5.1. Melt flow index, MFI

Reinforced TPE melt flow index values were measured by a melt flow indexer Ceast 6542/002 Melt Flow T.Q., at specified temperature and load for each TPE composite, namely:

- TPU composites at 2.16 kg at 200°C and SBS composites at 5 kg at 190°C.

Also pure TPU and SBS MFI were measured for comparison. Flow index (FI), grams per reference time is given by:

$$FI(T,M) = \frac{S \times m}{t} \text{ (g/10min)} \quad (4.1)$$

Where, T is test temperature, in Celsius degrees; M is the nominal weight, in kg; S is the reference time, in seconds; m is the average weight mass of the extruded segments obtained, in grams and t is the period of time between two cuts that determines a extruded segment in seconds. [8]

4.5.2. Mechanical characterization

4.5.2.1. Tensile tests

Tensile test specimens shapes (50 x 10 x 4 mm with 0,7mm thickness) were cut from the compression moulding plates (Figure 4.4) and tested. The standard mechanical tests were conducted according to ISO527- 2:1993. Tests were performed in a universal testing machine Instron type 4505 in a controlled environment (at 23°C and 55% relative humidity) and at crosshead velocity of 10mm.min^{-1} (nominated strain rate of 6.7x10 $^{-1}$ s^{-1}) until break.

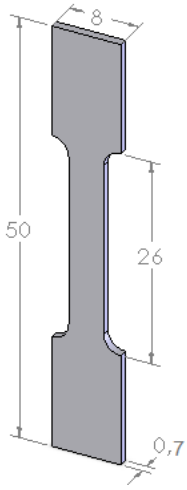

Figure 4.4– Tensile test specimens geometry (in mm).

Grip displacement (corresponding to the rectangular parte of tensile bar) was used to determine stretching ratio, $\lambda=(d+L_0)/L_0$, where, d is the displacement (mm) and L_0 (mm) is the initial clamp distance. Engineering stress was determined as $\sigma = F/A_0$ (MPa) where, F is the force and A_0 is initial specimen cross-section. Engineering strain was determined by $\varepsilon = d/L_0$ (mm/mm). The obtained

machine output curves were converted in the normalized stress-strain curves (normalized stress versus Ln λ) where, normalized stress is equal to engineering stress multiplied by stretching ratio (MPa).

Modulus, E_1, was determined by the secant modulus at 1% strain. Modulus, E_2, was determined by the tangent to curve as schematized in figure 4.5. The Young's modulus (E), yield stress (σ_y), stress at break (σ_b), yield strain (ε_y) strain at break (ε_b), were obtained directly from the force–displacement curves. Yield energy (U_y) was obtained by integration of area under the stress-strain curve in range of strain at zero till yield point. Energy at break (U_b) was assumed as the area under the stress-strain curve from strain at yield till break. At least six specimens per mechanical measurement were used, with estimated error/uncertainty not exceeding 10% in the data.

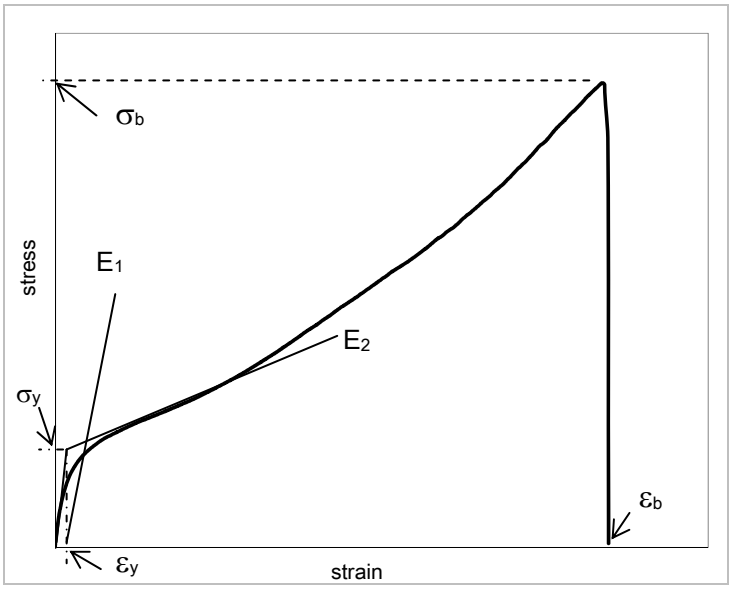

Figure 4.5 - Conventional for evaluating mechanical properties

In order to obtain more precise measurement during the test and hence an accurate assessment of the modulus, extensometers are normally used attached to the specimen. Because the maxims distance for the available extensometer for INSTRON was 50 mm with only 25mm range grip distance (not enough for specimens), it was impossible to follow the specimen strain. Therefore the use of extensometer was put aside, even knowing that this will affect the precision of the modulus determination and not allowing an accurate description of the beginning of the σ–ε curves.

After tensile tests, the morphology of the deformed area of the specimens was also analyzed.

4.5.2.2. Hardness

A Shore hardness tester (model D-7938 Oberdischingen shore A) manufactured by Bareiss- prüfgeräte, was used to measure the relative hardness of the TPE composites. The test method is based on the penetration of a specified indenter forced into the material under specified conditions. Tested specimens were composed of plied pieces to obtain the minimum thickness required, at 23°C and RH ± 50% according to ASTM 2240-05, with the surfaces of the plied specimens in complete contact. The lateral dimensions of the specimen were 12 mm from every edge. The specimen was placed on a hard, flat surface and the pressure foot of the instrument was pressed onto the sample. The hardness was red within one second after the pressure foot was in firm contact with the sample.

4.5.3. Thermal Characteriaztion

4.5.3.1. Thermagravimetric analysis, TGA

TGA was performed in nitrogen atmosphere with a TGA TA Instruments Q500. The sample was heated from 30°C to 800°C at a rate of 5°C.min^{-1}. The initial temperature of weight loss for the first and second step was denoted T_{d1} and T_{d2} and the corresponding temperatures at the maximum rate of weight loss of were denoted $DTG1_{max}$ and $DTG2_{max}$, respectively.

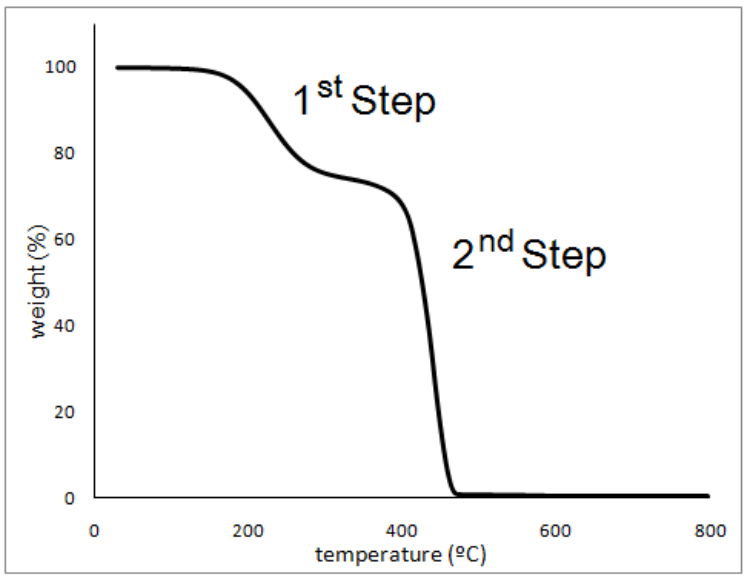

Figure 4.6 – A two steps TGA characteristic curve of a thermal decomposition reaction.

4.5.3.2. Differential scanning calorimetry, DSC, studies

The soft segment glass transition temperature ($T_{g,SS}$), hard segment glass transition temperature ($T_{g,HS}$), hard segment melting point ($T_{m,HS}$) of the neat and the TPE composites, and their respective enthalpies, were determined using a DSC Q20 Ta Instruments.

In order to obtain reproducible results for comparison, the DSC specimens had approximately the same weight (around 10 mg), 40 ml aluminium pans were used. An empty pan was used as reference. The test began with an initial temperature of - 80°C up to 200°C, at a heating rate of 20°C.min^{-1}. Then cooled to - 80°C and reheated ate the same rate to200°C. The 2nd sweep was performed in order to eliminate thermal history of the specimens. This way, it is guaranteed that all specimens are tested in the identical conditions, and fully understand the influence of fillers on morphology of TPEs. The same equal experimental procedure was always used in the measurements.

4.5.3.3. Thermal conductivity, λ_c

Thermal conductivity measurements were conducted by direct method with Alambeta equipment, used to measure textile, metal polymers, etc. [9] The used equipment, quickly measures all thermal properties of constant and transitory states of material. [9] The equipment simulates the heat flow. The sample is place on the base of the plate at T_0 temperature (cold), and measurement plate in contact with the sample. [9] After the heat is transfer through the sample is detected by a sensor and registered. The thickness, h, is automatically measured under constant pressure. [9] The recommended measure area is ± 100 mm^2 and 0.5 to 10mm of thickness. The samples area was ± 90 mm^2. The λ_c [W/m.K], can be acquire through the constant heat flow, located on the end of the heat flow base. [9]

4.5.4. Flame resistance

To evaluate the effect of reinforcing fillers on burning properties, the specimens were tested in a horizontal burn – UL 94HB tests, conducted according to ASTM D635 – 03. The principle consists on measuring the burning rate in horizontal position, and subjected to a pilot flame. [10] Burning rate, in mm/min, between 25 and 100 mm length was measured. Tests were conducted at humidity and controlled temperature (23°C e 50% HR). Specimens were: l= 125; b=13; d= ±0.7 (mm). The results

should be intended to serve as a preliminary indication of their acceptability with respect to flammability for a particular application. Linear burning rate (V) for each specimen where the flame front reaches the 100 mm reference mark, was calculated by:

$$V=60L/t \tag{4.2}$$

Where, L is the burned length, in millimeters, and t is the time, in seconds.

4.5.5. Electrical measurements

Resistivity measurements were performed on TPU with CNF, TPU with HSCB and SBS with HSCB specimens with two-point contact method at 23 ± 2 °C and 50 ± 5 % relative humidity. A constant voltage was applied, and an automated Keithley 487 picoammeter/voltage source, [11] (Figure 4.7) was used for measure the low currents. The surface specimen was cleaned by rubbing with fuller's earth (hydrated magnesium-aluminium silicate) and distilled water according to ISO 3915:1981, then allowing it to dry. After cleaning, specimens are coated by chemical vapor deposition (CVD) creating two golden layers prior to tests to glue the copper wires, theses ensuring good electrical contact. The distance between electrodes is larger than the radius of contact area. [12,13] The resistivity (R) was calculated through the slope of I-V curves, with Ohm's law. For surface measurements configuration, electrode had 6 x 2 mm length and 1 mm distance (Figure 4.8 a)). For volume measurements configuration, electrode had 5 mm radius and 0.075 mm distance (samples thickness)(Figure 4.8 b)).

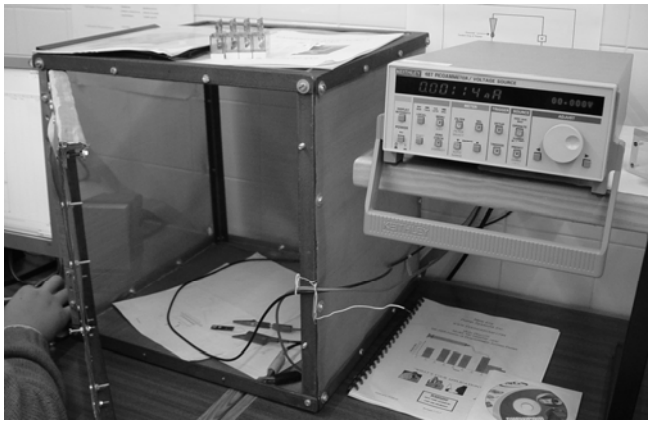

Figure 4.7 - Automated Keithley 487 picoammeter/voltage source.

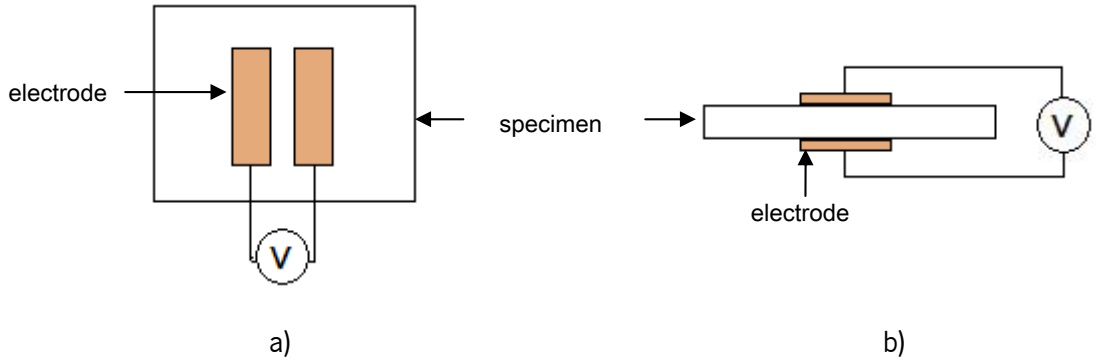

Figure 4.8 – Electrical measurements a) surface electrode configuration; b) volume electrode configuration.

4.6. REFERENCES

1. www.aerosil.com
2. www.sud-chemie.com
3. www.degussa-fp.com
4. www.electrovac.com.
5. www.hoben.co.uk
6. http://www.palabora.com
7. Breuer O., Sundararaj U., Polymer Composites. Vol.25 (2004), p.630.
8. NP 2914 - Determinação do índice de fluidez dos termoplásticos.
9. "Manual do instrumento Alambeta", D.T., Universidade do Minho.
10. ASTM D 635 03-Standard test method for rate of burning and or extent and time of burning of plastics on horizontal position.
11. www.keithley.com
12. Gutiérrez M. P., Li H., Patton J. - Thin Film Surface Resistivity. Materials Engineering, Proc. Inst. Radio Engrs. Vol 42 (2002), p. 420.
13. Gutiérrez M.P., Li H., Patton J. - Surface Resistivity: Measurement and Common Applications for Semiconductors and Insulators. In MATE210 – Fall. 2002.

CHAPTER 5

RESULTS AND DISCUSSIONS

This chapter covers the obtained experimental results in four sections: microstructural/morphological; mechanical; anti-static-electric and thermal characterization. A preliminary morphological analysis establishes some evident correlations between the blending process and the dispersion/aggregation of particles. The mechanical, thermal and electrical properties are used thereafter in order to quantify the relative significance of each particle on the TPE matrix. The particle-structure-properties relationships are established.

5.1. RESULTS AND DISCUSSIONS

The effect of fillers incorporation on TPEs was evaluated by comparing neat TPE and composites system.

5.1.1. TPEs identification by FTIR

TPU typical main functional groups were assigned and demonstrated in Figure 5.1. The peak around 3390 cm^{-1} and 1536 cm^{-1} was attributed to stretching vibration of amine groups N-H, which is due to the hydrogen bonded -NH in the urethane linkage. Typically, the -NH groups in the urethane linkage form hydrogen bonds with the carbonyls of the urethane linkage in the hard segment. The -NH groups are also able to form hydrogen bond with the carbonyl of ester-polyol in case of ester-TPU. Careful examination of -NH and carbonyl peaks in the FTIR spectra can give some information on the morphology of the hard and soft segments in the polyurethane as done by Pattanayak and Jana.[1] Carbonyl -C=O stretching are shown at 1730 cm^{-1}. The absorption bands around 2964 cm^{-1} are attributed to the asymmetric and symmetric stretching vibration of CH_2 bond. Peak 1602 cm-1 is attributed to C=C group and 905 cm^{-1} to C-O bonded.

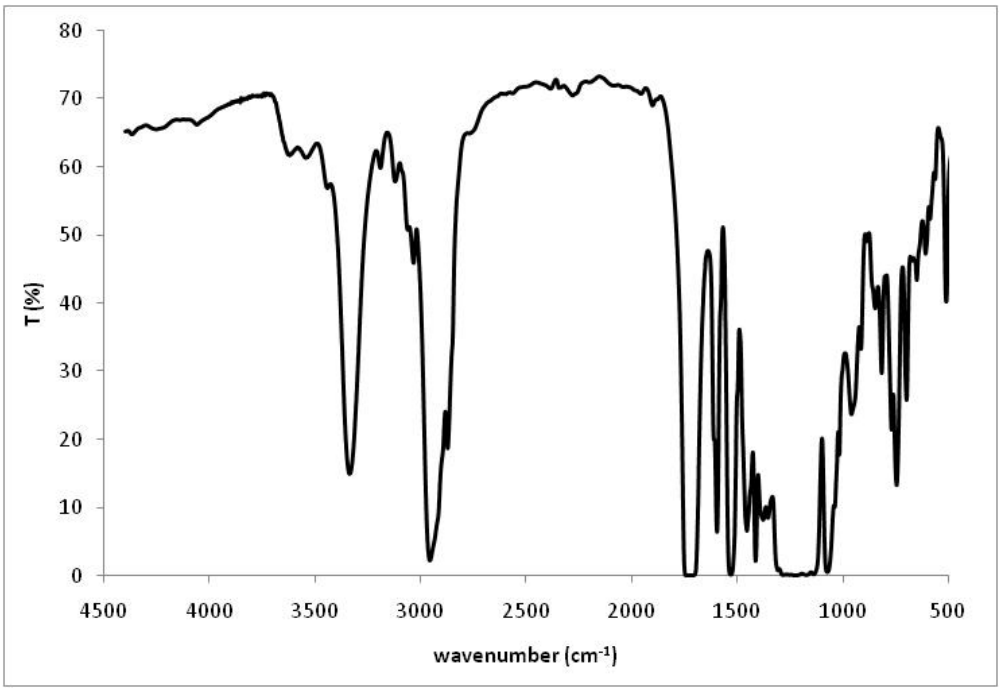

Figure 5.1 - FTIR Spectra of neat TPU.

In Figure 5.2 is shown the spectra for SBS polymers. The bands at around 2922 cm^{-1}, 1456 cm^{-1} and 700 cm^{-1} are attributed to stretching vibrations of C-H band. The absorption bands around 1642 cm^{-1} are attributed to stretching vibration of C=C.

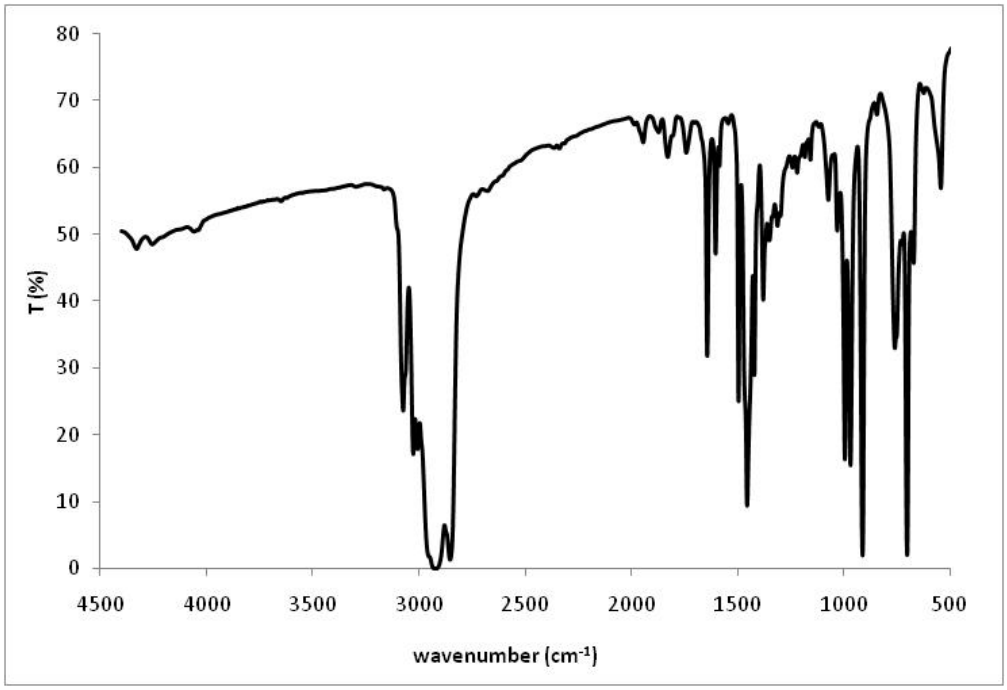

Figure 5.2- FTIR Spectra of neat SBS.

In the Annex III are shown the FTIR-spectra for all the TPE composites. No new absorption bands were observed, but existing bands intensity has increased, demonstrating some degree of interaction between fillers and polymers matrix.

5.1.2. Microstructural analysis

The macroscopic observation of the obtained compression moulded plates (Figure 5.3 and Figure 5.4 are an example of the obtained composite systems) revealed that the miniature mixing device has a good dispersive mixing capability, resulting in an uniform dispersion of microfillers in TPE matrices. Furthermore, the addition of NS did not affected the TPU transparence (agglomerate sizes smaller than the light wavelength.

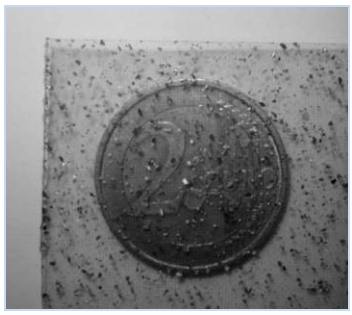

Figure 5.3- TPU plate with microsized vermiculite (Hoben).

Figure 5.4- TPU plate with nanosized nanosilica Aerosil 200.

5.1.2.1. Optical microscopy, OM

In a first assessment by optical microscopy, Figure 5.5 shows a good distribution and a size variation of HSCB particles (from 20 to 50 μm), reveling that the dispersion process energy was not capable of breaking all the characteristic HSCB aggregates.

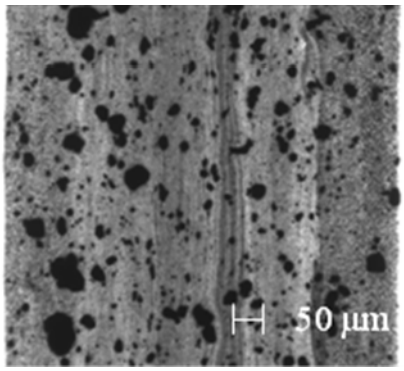

Figure 5.5 - OM images of TPU+HSCB surface cross-section (magnification 10 x).

Figure 5.6 depict a OM images of the neat SBS.

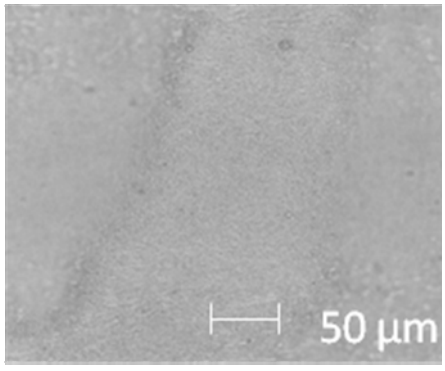

Figure 5.6 - OM images of neat SBS surface cross-section(magnification 20 x).

Figure 5.7 a) shows once again a good distribution of the HSCB in the SBS matrix. As occurs with HSCB filled TPU, the presence of HSCB larger aggregates is observed. Figure 5.7 b) and c) reveal a more coarse image compared to neat SBS (Figure 5.6), however, particles agglomerates were not detected for these nanofillers.

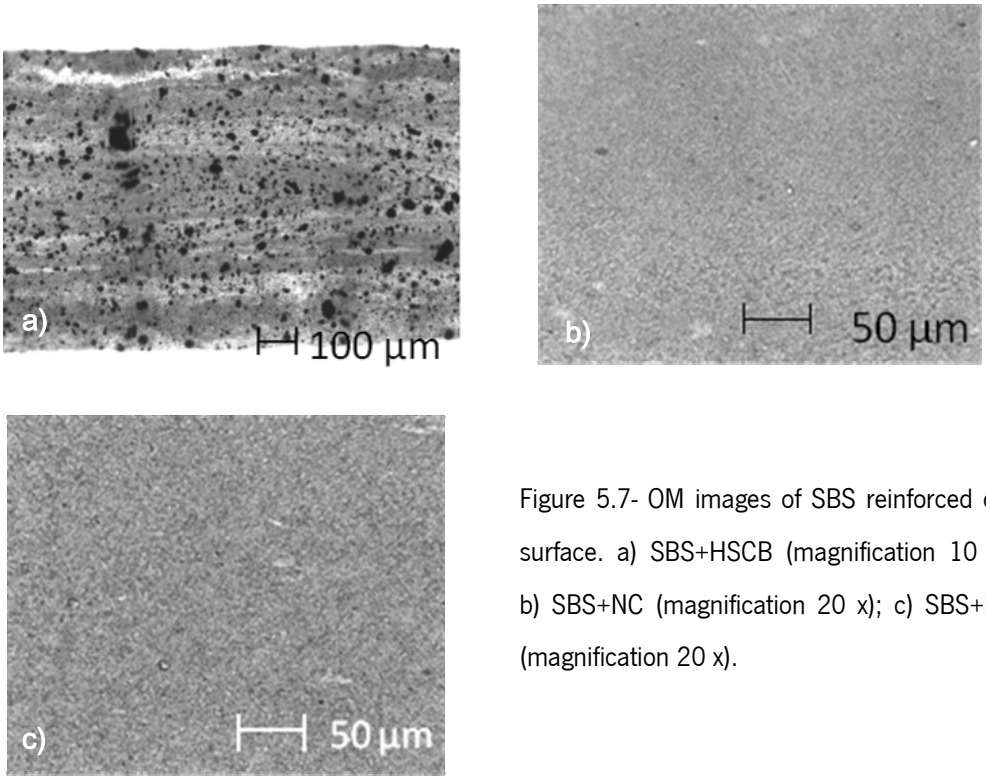

Figure 5.7- OM images of SBS reinforced cut surface. a) SBS+HSCB (magnification 10 x); b) SBS+NC (magnification 20 x); c) SBS+NS (magnification 20 x).

5.1.2.2. Scanning electron microscopy, SEM

The microstructure of specimens was observed by SEM at higher magnifications and shown in Figures 5.8 to 5.14. Figure 5.8 shows the fracture surface of neat TPU (for comparison). As presented in Figure 5.9a) the HSBC particles are very small with 30 nm medium size and fairly good distributed on the TPU matrix. Occasionally, agglomerates of HSCB particles with 90 nm size were detected. As observed previously in OM characterization, the size variation of HSCB particles reveals that the dispersion process energy was not capable of breaking all HSCB aggregates. In Figure 5.9b) an uniform dispersion of CNF in TPU matrix, with absence of agglomerates and porosity, is shown. No appreciable breakage of nanofibers could be observed. Measured nanofibres diameter is between 120 and 400 nm, much higher than the average diameter of 80 – 150 nm indicated by the supplier. This higher diameter suggests that some polymer covers the nanofiber surface, indicating good interaction at the fiber-

polymer interface resulting in a good phase adhesion between polymer and CNF. The SEM pictures depict a fairly good distribution of fillers in the matrix.

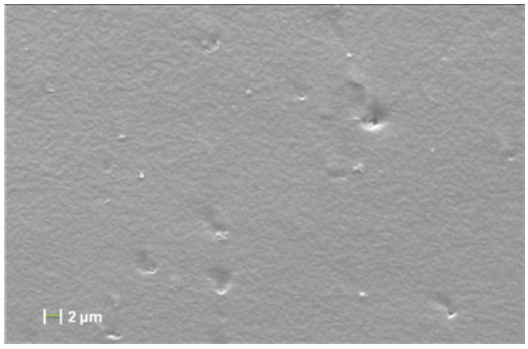

Figure 5.8- SEM images of TPU fractured surface (magnification 2000 x, 15kv).

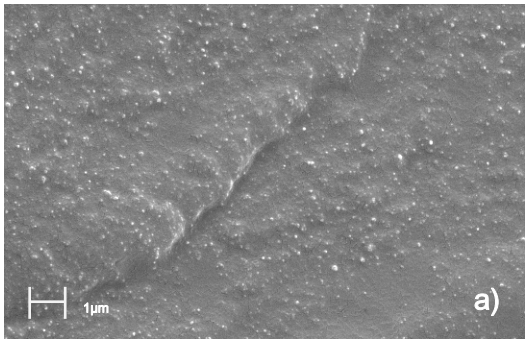

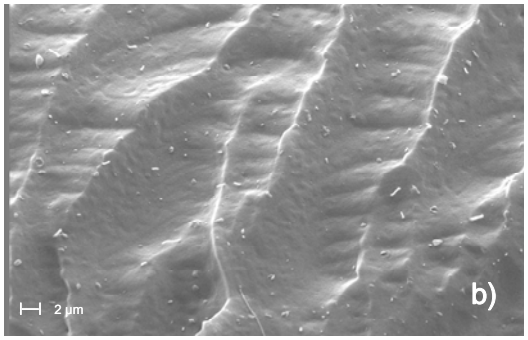

Figure 5.9- SEM images of TPU reinforced fractured surface. a) TPU+HSCB (magnification 20 000 x, 10kv); b) TPU+CNF (magnification 2000 x,15kv);

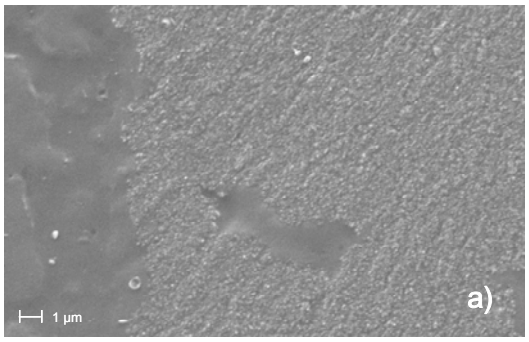

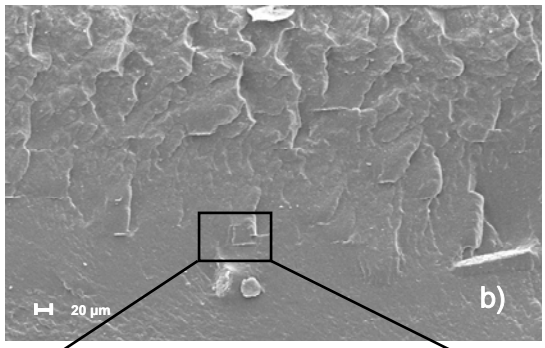

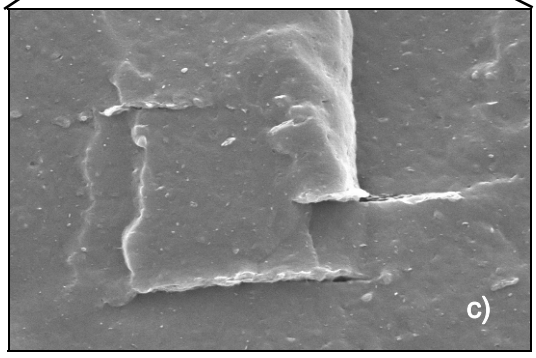

Figure 5.10 - SEM images of TPU reinforced fractured surface. a) TPU+NS (magnification 5000 x,15kv); b) TPU+NC (magnification 200 x, 15kv); c) detail of image 5.8b) showing a tactoid with ± 1µm (magnification 2000 x, 15 kv).

Figure 5.10 b) shows agglomerations of NC know as tactoids. The dispersion and exfoliation of nanoclays in a polymer matrix proved to be a complex chemical/physical process. The dispersion level depends greatly on extrinsic parameters such as screw configuration,[2,3] melt temperature and screw rate[3,52], as well as on intrinsic parameters, as compatibility between the matrix and the filler [2,3] and surface free energy [3] of the particles. [4,5] For the specific TPU nanoclay composite, the mixing time should be longer for better intercalation/exfoliation.

The Figure 5.11 depict the good adhesion between the TPU and VCC, as well as the TPU and VCE, with bridges formation (Figure 5.11 b).

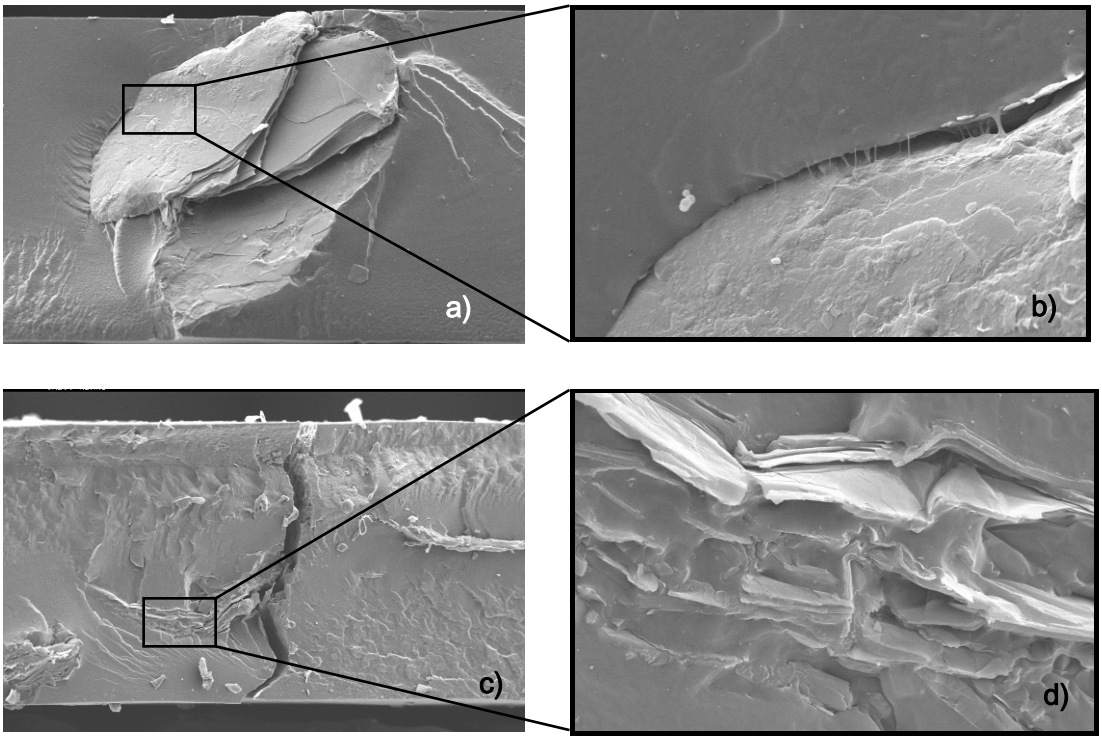

Figure 5.11 - SEM images of TPU reinforced fractured surface. a) TPU+VCC (magnification 140 x, 15kv); b) Larger resolution of detail on figure 27.a) (magnification 2000 x,15kv); c) TPU+VCE (magnification 140x, 15kv); d) Larger resolution of detail on figure 27 c) (magnification 1000x,15kv).

Figure 5.8 shows the fracture surface of neat SBS (for comparison).

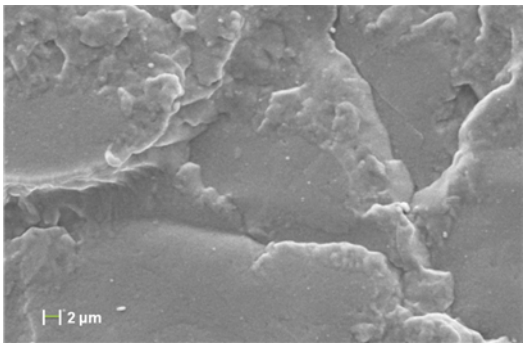

Figure 5.12 - SEM images of SBS fractured surface. (magnification 2000x, 15kv).

Similar results were obtained for SBS composites. In Figure 5.13a), the HSBC particles are very well distributed and particle size variations is observed (agglomerates with c.a. 100 nm size). In Figure 5.13b), contrary to what happened with NS filled TPU, no coarse grains are observed. Surprisingly, the NC tactoids observed in the TPU systems are not so pronounced in SBS composites, as presented in Figure 5.13c). It is worth noting that the mixing conditions were equal for both matrices, and equal amount of NC were used, but SBS has chemical differences and different viscosity that could helped in a more effective intercalation/exfoliation.

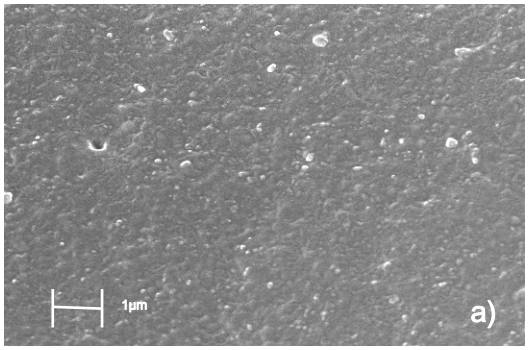

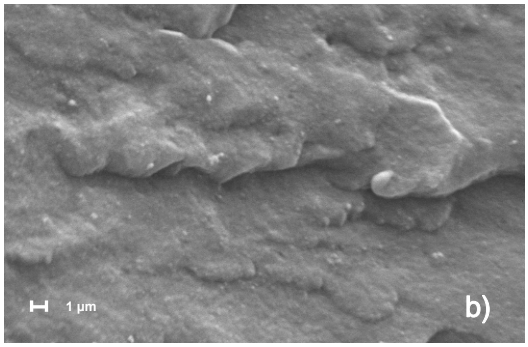

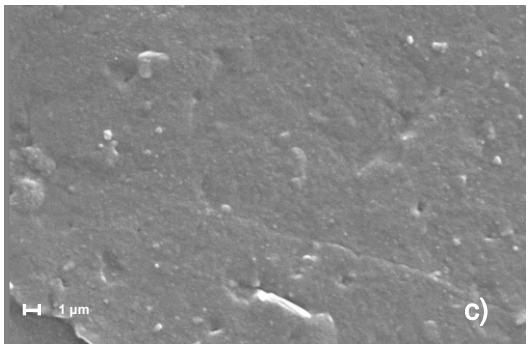

Figure 5.13 - SEM images of reinforced SBS fractured surface. a) SBS+HSCB (magnification 5000x, 15kv); b) SBS+NS (magnification 5000x, 15kv); c) SBS+NC (magnification 5000 x, 15kv).

A good adhesion between SBS and VCC and VCE is shown in figure 5.14.

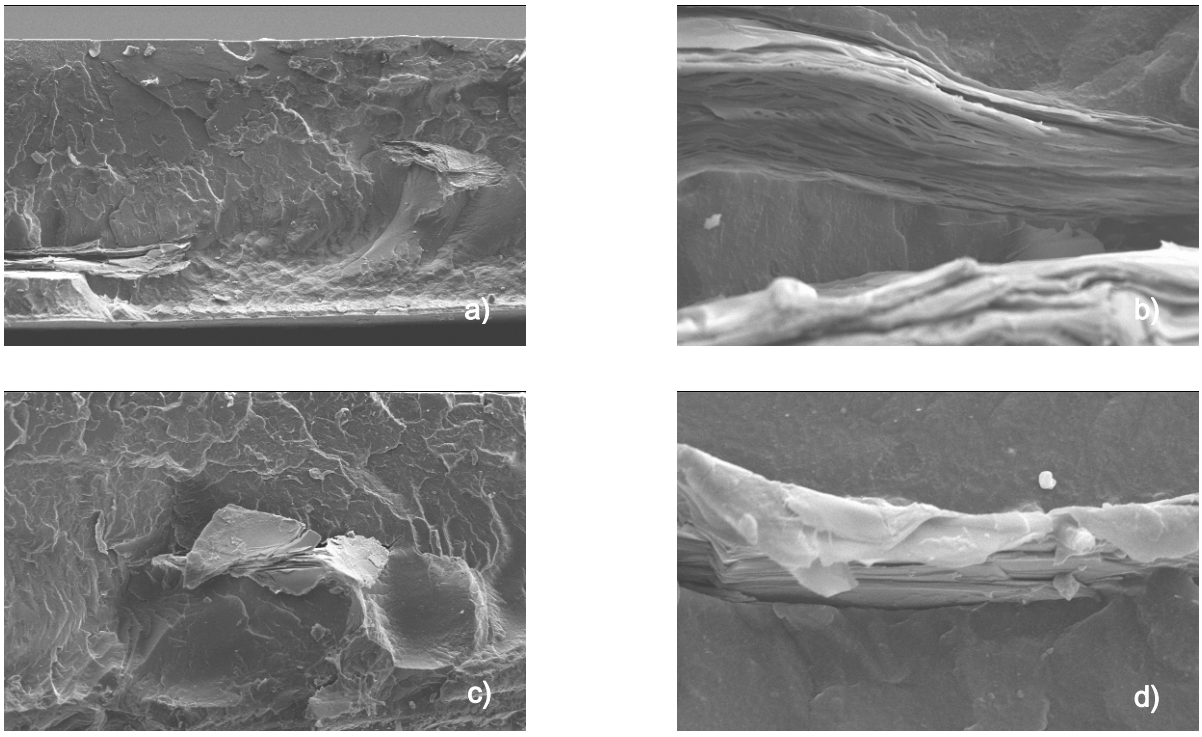

Figure 5.14 - SEM images of reinforced SBS fractured surface. a) SBS+VCC (magnification 140x, 15kv); b) SBS+VCC (magnification 2000 x, 15kv); c) SBS+VCE (magnification 140 x, 15kv); d) SBS+VCC (magnification 2000 x, 15kv).

Summary

Optical microscopy analysis contributed for a preliminary validation of the dispersion capability trough the adopted mixing procedure. Good distribution was achieved, but not of a complete de-agglomeration in the case of HSCB filled TPEs. SEM images corroborate OM analysis, were incomplete HSCB particles de-agglomeration reflected by size variation is once again observed. Fully NC exfoliation wasn't achieved. Dispersion of the nanoparticles showed that can be difficult because they have tendency to aggregate.

5.1.2.3. Melt flow index, MFI

Figure 5.15 resumes the overall variation of the melt flow index of the TPE versus TPE composites. A sudden small increase in value torque is seen with the joining of nanofillers, as a result of the viscosity increasing due to the high superficial area of the fillers. In comparison with the neat TPU, only CNF and VCE had is MFI increased. This may indicate promoted slippage by the CNF and VCE fillers. The MFI results of TPU filled CNF may also be explain by the fact of the added CNF being a masterbatch, with

includes another type of TPU which could have a higher MFI. HSCB, NS, NC and VCC had TPU MFI decreased. This could be explained by network formations. NC filled TPU shows the higher MFI drop. Neat SBS clearly shows higher flow index than neat TPU. With exception of NS, the micro- and nanofillers incorporation had highly increased SBS MF, reveling good. filler-polymer interaction. NC filled SBS shows the higher MFI increase of all composites systems, unlike what happened to filled TPU. Summarizing, same fillers in the different TPEs matrix had different effects that will be reflected in the melting process and composites properties.

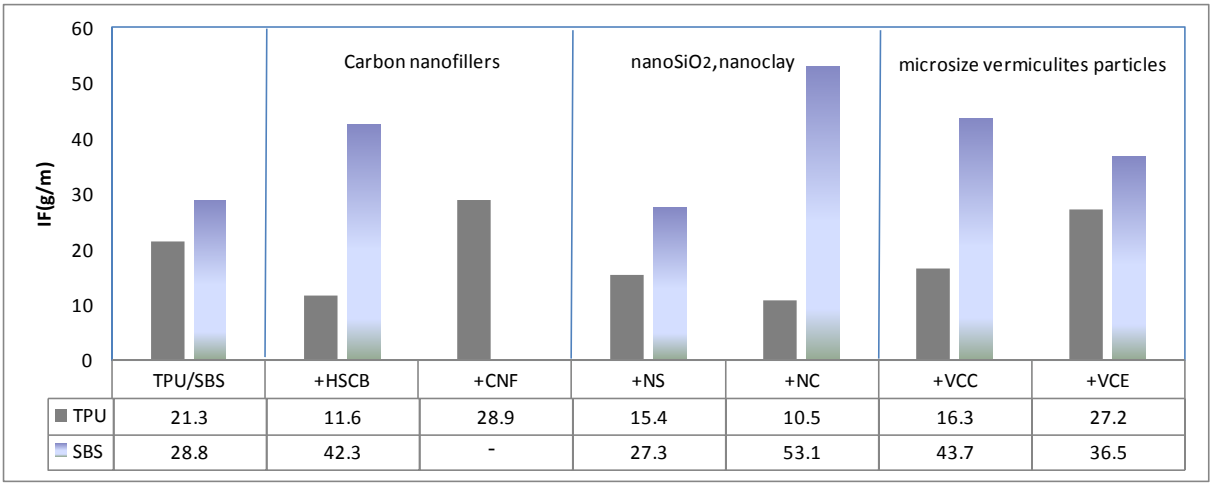

	TPU/SBS	+HSCB	+CNF	+NS	+NC	+VCC	+VCE
TPU	21.3	11.6	28.9	15.4	10.5	16.3	27.2
SBS	28.8	42.3	-	27.3	53.1	43.7	36.5

Figure 5.15 – Neat and TPEs MFI composites results.

5.1.3. Properties characterization

5.1.3.1. Mechanical characterization

The effect of the reinforcing fillers on TPE mechanical behaviour is plot in Figure 5.16 to 5.23. In each TPE system, a representative curve was selected and plotted for comparison. As observed from Figure 5.16 and 5.17, the micro - and nanoreinforced TPU shows similar behavior, but withstand more stress and strain (in some cases by more than 300%). This behavior indicates that TPU is more deformable when reinforced. Micro- and nanofillers have increased TPU ductility. The SBS presents not so notorious improvements with stress behavior variations. The effect of incorporation of the fillers is different depending upon the TPE matrix.

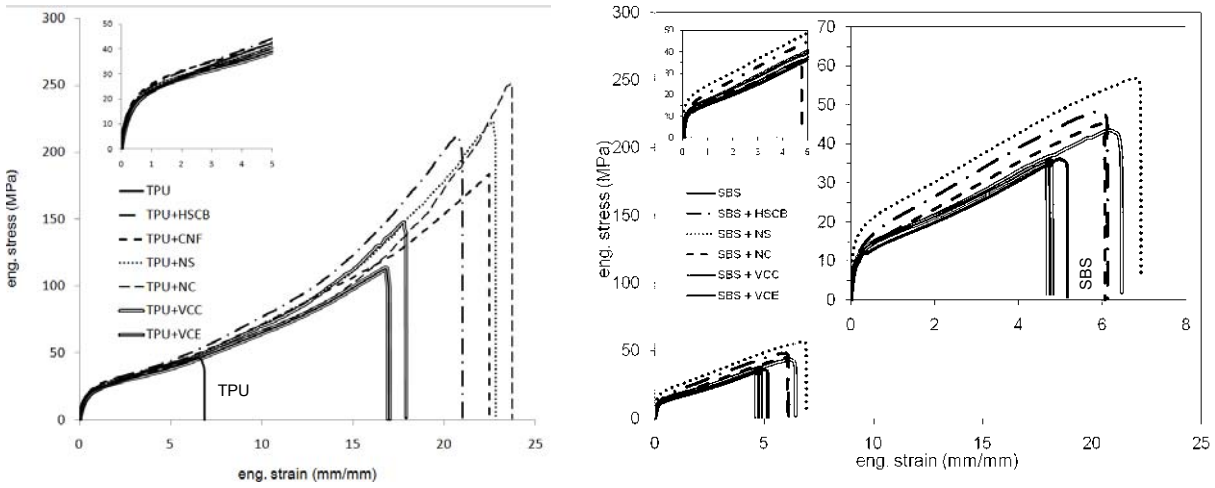

Figure 5.16- Stress-strain curves.

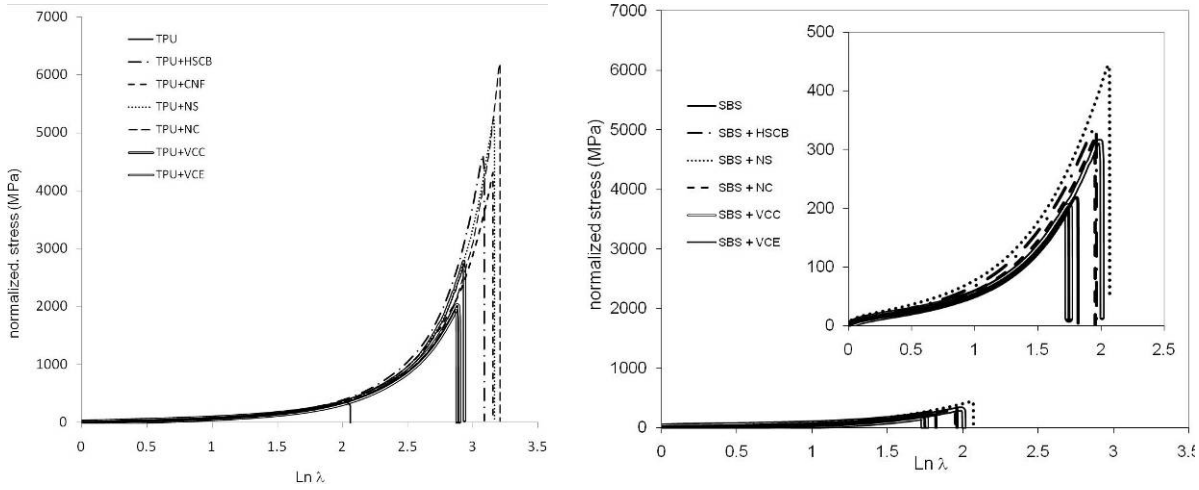

Figure 5.17 - Normalized stress-strain curves.

The following Figure 5.18 to Figure 5.23 depicts the effect of the type of reinforcement on the particular mechanical properties of the composites. These results revealed that the incorporation of micro- and nanosize particles increases TPEs mechanical properties, with great influence on the TPU and not so notorious effect on SBS.

Compared to the neat TPU, and with the exception of TPU+HSCB and TPU+NS composites, the TPU composites modulus, E_1, show improvements. Surprisingly, TPU+CNF composite shows an enhanced of E_1 of more than 100% (Figure 5.18). This higher modulus of the nanocomposites reflects the higher interfacial area and aspet ratio of CNF that allows a larger contribution of the stiffer particles to the modulus. It also anticipates the possible formation of a filler network that withstands the initial deformations. The modulus clearly increased after CNF, NC, VCC and VCE incorporation, indicating that

fillers had a good adhesion to the TPU matrix. On the contrary, the SBS composites show no significant enhancements upon E_1.

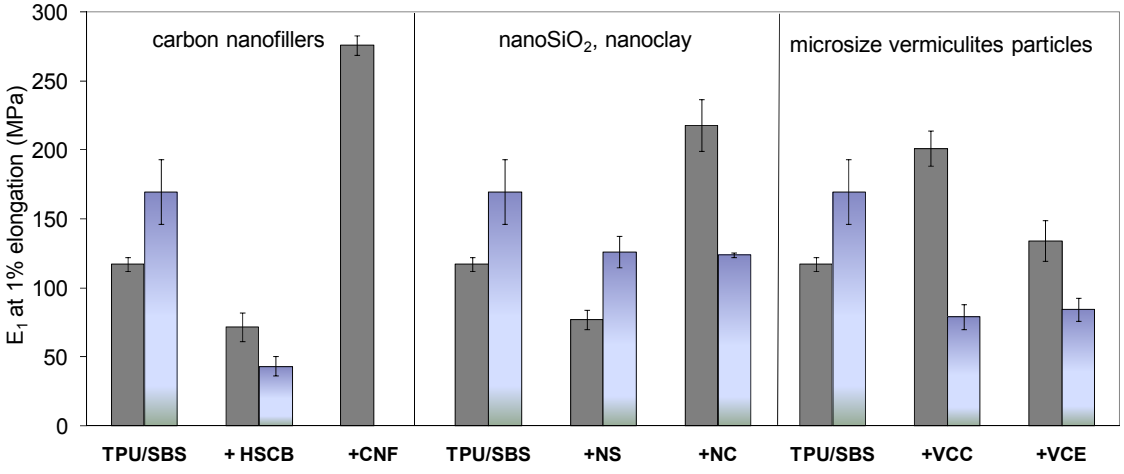

Figure 5.18 – Variations of E_1 with the incorporation of micro and nanosized in TPEs.

On the other hand, it can be seen in Figure 5.19 that all composites show E_2 enhancement. For TPU matrix, NS and NC nanoparticles presence shows the highest enhancements by more than 100%. The good dispersion of NS observed in SEM, and this materials high surface energy could explain this improvement. All TPUs composites have presented E_2 improvements. A possible explanation for this behavior may be the formation of crosslinks by the fillers that give a higher stress levels.. Simultaneously the fillers promote easier matrix chain sliding increasing TPU deformability, As reported by Shen et all.,[6] the introduction of clay layers induced the crystallization of PU hard segments. This change of crystallization may lead to changes on the mechanical properties. This may anticipate that for the case of TPU fillers may be preferentially located in the TPU hard domains.

With exception of VCC and VCE microparticles, all SBS composites show improvements on E_2. The nanosized particles are again affecting the formation of crosslinks by the fillers that give a higher stress levels. For the VCC and VCE the micrometric size of the particles creates stress concentration leading to an earlier rupture of the matrix.

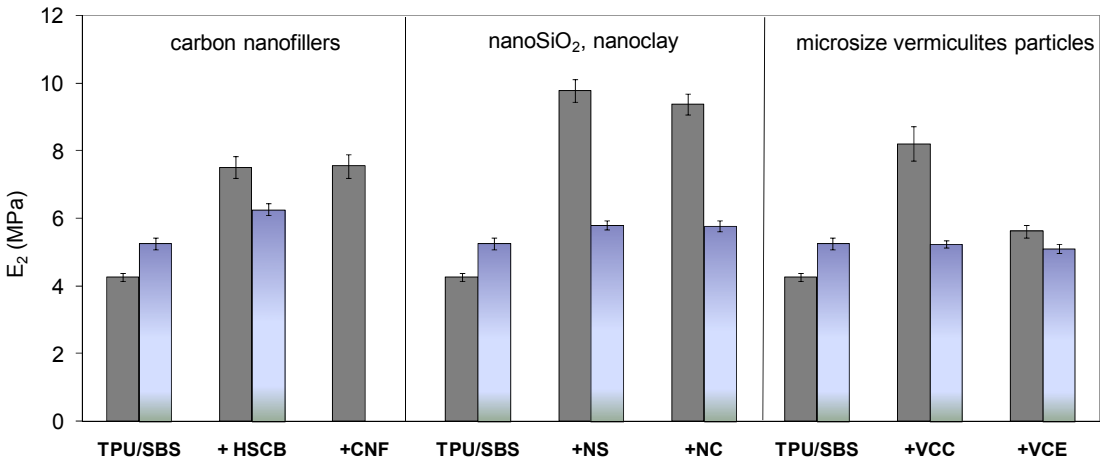

Figure 5.19 – Variations of E_2 with incorporation of micro and nanosized reinforced in TPEs.

Figures 5.20 and 5.21 show that for TPU both micro- and nanofillers contributed for a small improvement upon the yield stress and yield strain, σ_y and ε_y, respectively. SBS composites show not so notorious improvements, the results indicating only a small contribution to strength by filler incorporation. Even the presence of VCC and VCE affects negatively SBS properties at yield.

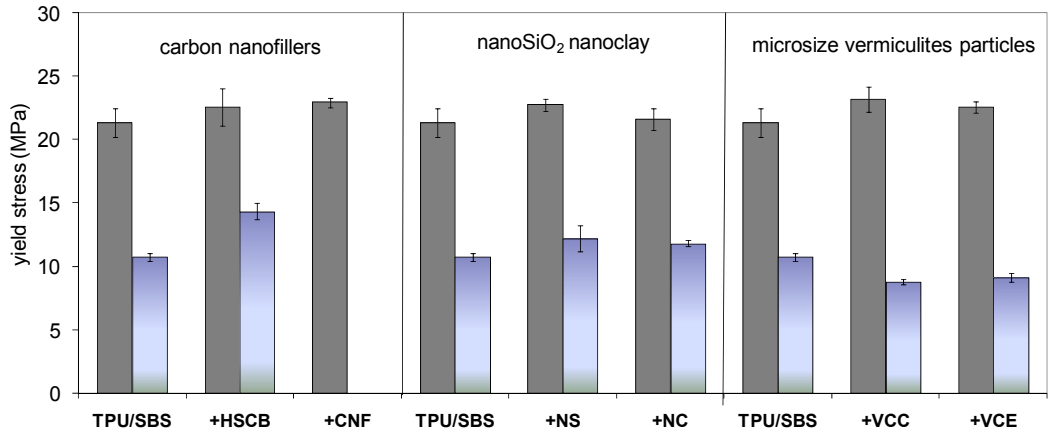

Figure 5.20 – Variations of yield stress, σ_y, with incorporation of micro and nanosized reinforced in TPEs

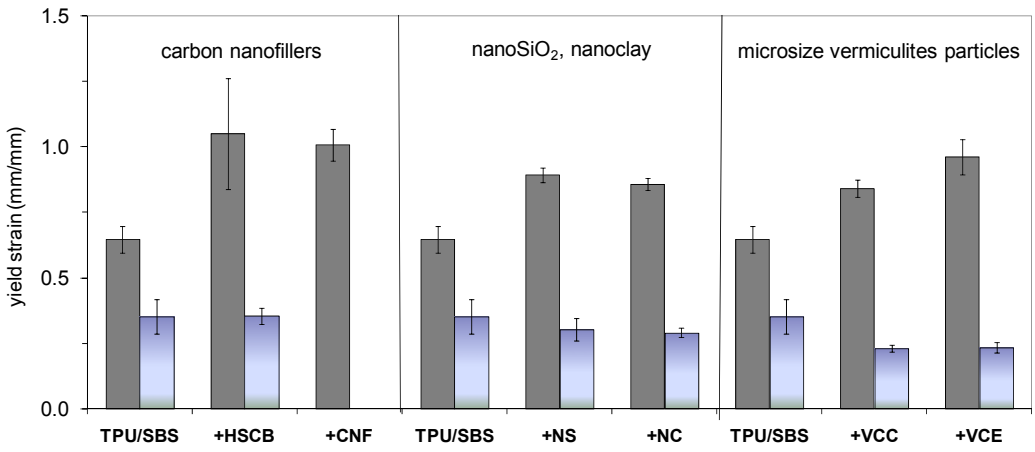

Figure 5.21 - Variations of yield strain, ε_y, with incorporation of micro and nanosized reinforced in TPEs.

Figures 5.22 and 5.23 further shows the effect of micro- and nanoparticles on the TPEs tensile behavior at break. The TPU composites had the most notorious effect with significant improvements upon the properties at break (stress and strain). The HSCB, CNF, NS and NC incorporation increased both the stress and strain at break: by ± 90% for HSCB, CNF and 480% and 372% for NS and NC, respectively. This enhancement of mechanical properties is thought to be associated to a good nanofiller adhesion to TPU matrix, the formation of crosslinks and the easier macromolecular sliding. Previously in the MFI analysis, with the exception of the CNF filled TPU, these same fillers increased MFI suggesting a good filler-polymer interaction (Figure 5.15). Both the stress and strain at break of filled TPU are significantly increased, making it possible to add multifunctional behaviors with improved mechanical behavior.

With the exception of vermiculite fillers, the tensile properties of SBS slightly improved with the presence of nanofiller particles. The VC fillers have affected negatively the SBS deformability, and it is thought to be associated to the formed microsized particle. SBS strain at break is maintained with nanofillers incorporation making it possible to add multifunctional behavior without compromising deformability.

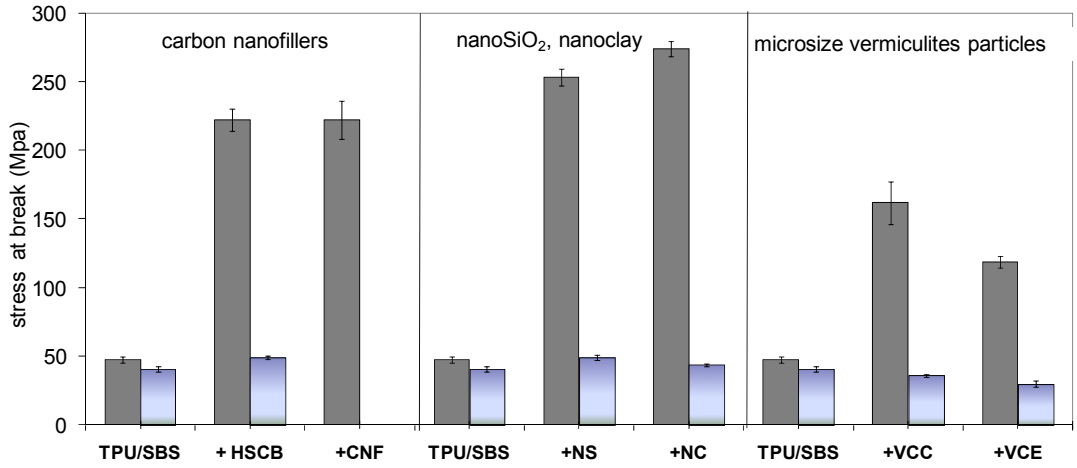

Figure 5.22 –Variations of stress at break, σ_b, with incorporation of micro and nanosized reinforced in TPEs.

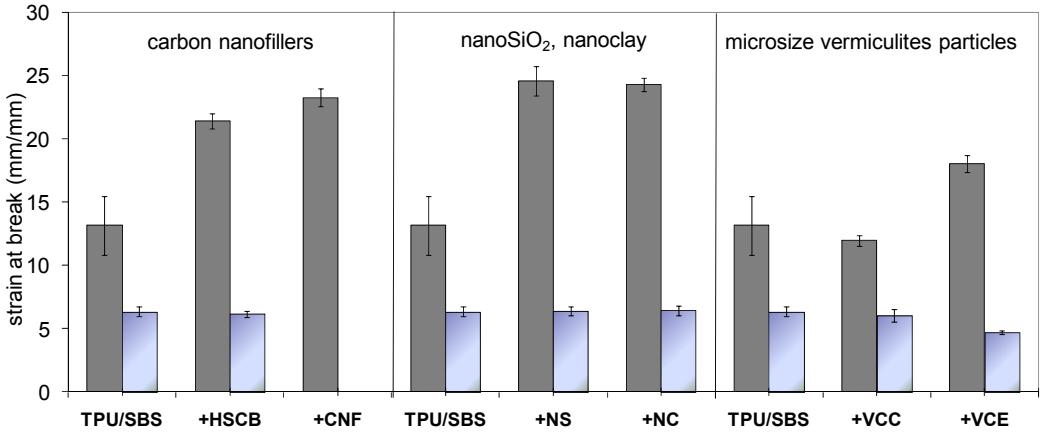

Figure 5.23 –Variations of strain at break, ε_b, with incorporation of micro and nanosized reinforced in TPEs

In the Annex IV are shown the yield energy, U_y, and energy at break, U_b, of the micro- and nanoreinforced TPE.

Further evidence for the significant mechanical behavior of TPE composites is provided by the representative SEM images of the fractured surface of the resulting tensile deformed specimens. As illustrated in Figure 5.24a) a massive matrix deformation of TPU filled with HSCB is observed; on image b) fibers maintain their good adhesion showing no voids around the nanofillers in TPU matrix, and there orientation is on drawing direction.

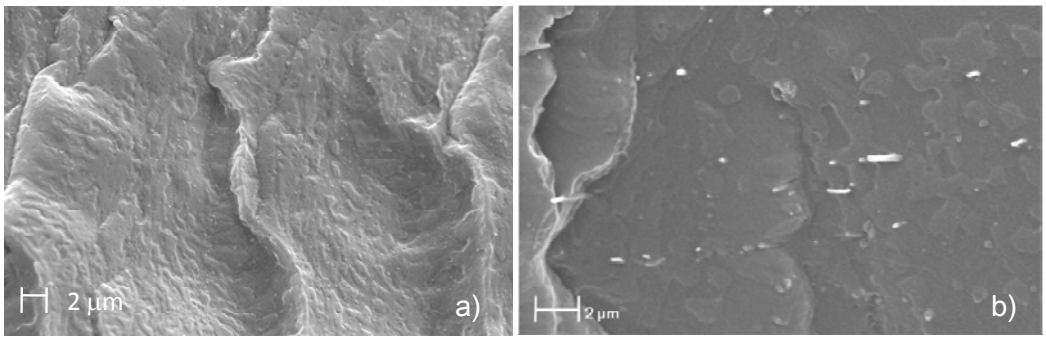

Figure 5.24- SEM images after tensile tests of fractured surface a)TPU+HSCB (magnification 2000 x,15kv); b)TPU+CNF (magnification 5000 x,15kv).

In Figure 5.25 some fibrillation is observed for NS-TPU systems. The fibrillation is a result of a good interfacial bounding between filler and the matrix, and the good dispersion of the filler [7], which reflects on mechanical properties improvements as demonstrated on the assessed tensile properties.

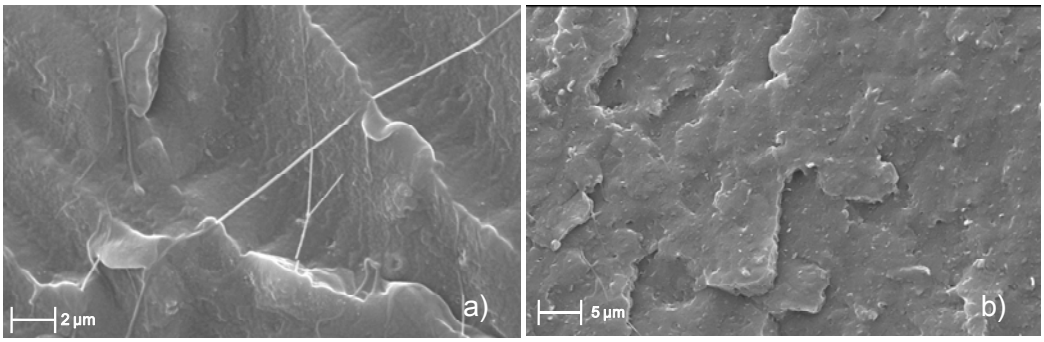

Figure 5.25 - SEM images after tensile tests of fractured surface a)TPU+NS (magnification 5000 x,15kv) ; b) TPU+NC (magnification 2000 x,15kv).

Summary

Considering the above discussions, filler particles strongly influence the polymer chain mobility. Microstructure evolution and resulting performance of these micro- and nanocomposites TPEs depend both on the composition of the matrix, as well as on the reinforcing particles. This explains the different results upon different polymer matrices. A good dispersion and lack of agglomerations have a positive effect on mechanical properties. This provides larger contact surface for the dispersed phase, avoiding local stress concentrations to be reflected on properties. Nevertheless, these TPE nanocomposites reveal clear improvements in initial modulus, ultimate strength and strain at break with the incorporation of such fillers without sacrificing the other mechanical properties.

5.1.3.2. Hardness

TPEs hardness measurements clearly indicate that TPU is a harder material than SBS. Table 5.1 summarizes the effects of the addition of micro- and nanoparticles on the TPEs hardness (see also Figure 5.26).

Table 5.1 - Effect of micro- and nanoparticles on the hardness of TPU and SBS.

Samples	Hardness (shore A)	Samples	Hardness (shore A)
TPU	64	SBS	58
TPU+HSCB	65	SBS+HSCB	60
TPU+CNF	60		-
TPU+NS	62	SBS+NS	58
TPU+NC	65	SBS+NC	58
TPU+VCC	60	SBS+VCC	54
TPU+VCE	57	SBS+VCE	55

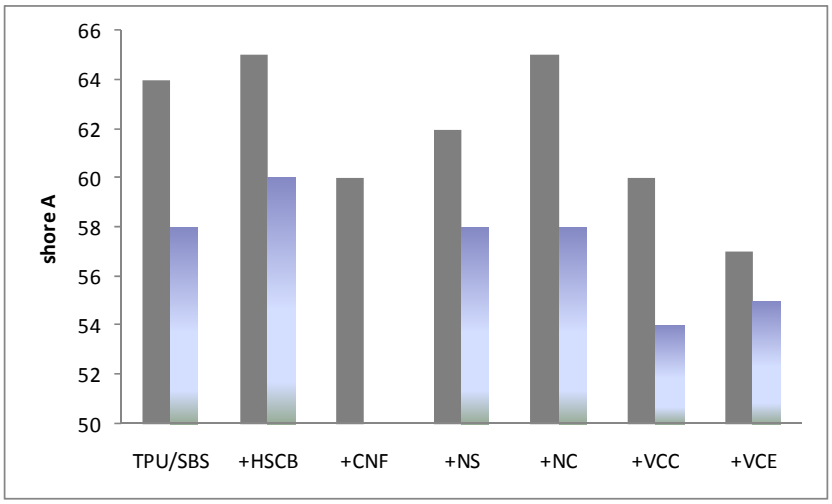

Figure 5.26 - Effect of micro- and nanoparticles on the hardness of TPU and SBS.

The results show that the incorporation of small amounts of HSCB into both TPE matrices led to an increase of hardness, suggesting some influence of these particles. When CB is dispersed inside the SBS matrix, a preferential interaction of the filler is expected with the soft segment, SS, phase, as observed in a previous study of PS–Polybutadiene blends [8]. This may explain the increase of hardness, as SS are more restrained. The same it is thought to happen for the TPU SS domains. Furthermore, the incorporation of filler seems to allow a high density of physical crossslinks, as already abovementioned. Interestingly the addition of NS and NC fillers had no effect on SBS hardness. The incorporation of CNF decreased slightly the TPU hardness, in spite of the increase on the initial

modulus (Figure 5.18). NS has also decreased TPU hardness as decreased the initial modulus (Figure 5.18). VC particles have decreased the hardness of TPEs. In some cases, VC decreases the initial modulus (e.g., SBS). Some sliding of fillers large tactoids may also induce a decrement upon composite hardness, mainly in case of good filler-matrix adhesion.

5.1.4. Thermal properties

5.1.4.1. Thermal gravimetric analysis, TGA

The effect of reinforced particles on the thermal stability of TPE was evaluated by TGA. The results for neat and reinforced TPEs are shown in Figure 5.27 and Tables 5.2 and 5.3. Figure 5.27 shows the mass loss variation with temperature. No expressive weight loss was register between the 30°C to 200°C. As reported by other researchers [6], the first degradation process corresponds to the release of the little molecules or unstable side chains, which will degrade at lower temperature. TPEs thermal degradation is a complicated process. It has been found that thermal degradation of TPEs occurs in two stages, [9,10] since hard and soft segments (HS and SS, respectively), respond differently at high temperatures. In TPU 1st step, decomposition of the HS occurs, involving dissociation of urethane from the original polyol and isocyanate. In 2nd step, deploy condensation and polyol degradation of the SS takes place. Therefore, 1st step can be associated to initial temperature of weight loss, T_{d1} of HS, while 2nd step can be related to T_{d2} of SS. [10-12]

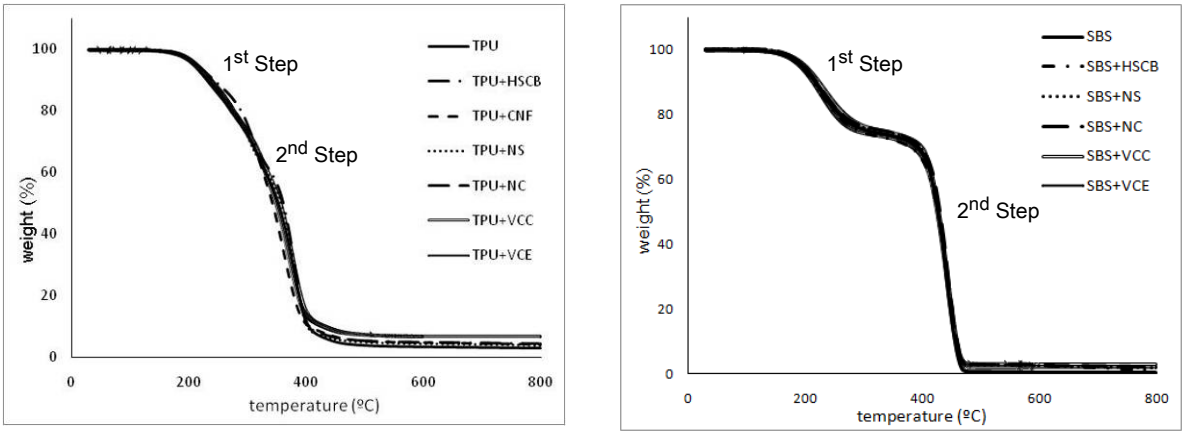

a) b)

Figure 5.27 – Mass loss a) TPU composites; b) SBS composites.

The TGA results for TPU composites are shown in Table 5.2. The first degradation of TPU occurred at 192 °C and the second degradation at 342 °C. As it can be noticed, HSCB and CNF affect differently TPUs hard and soft domains. The incorporation of HSCB didn't improve T_{d1}, but did improve T_{d2}, delaying it by ~12°C. This indicates that HSCB may preferably interact with the SS in polyurethane structure. The CNF presence has delaying the 1st degradation temperature by ~4°C, suggesting that the nanofibers interacted more with the TPU HS domains. Expectantly, the thermal stability is expected to improve with the incorporation of more thermally stable fillers such as HSCB and CNF. This was interpreted by: the adsorption of free radicals by the carbon fillers surface; [13] by the uniformly dispersed carbon nanofillers presumably providing higher thermo-oxidative stability to the polymers in the vicinity of the fillers surfaces; [10] by the enhancement of the thermal conductivity of the composite that can facilitate heat transport and thus increase its thermal stability [14]. Table 5.2 shows also the thermal stability improvement of TPU filled with NS and NC.

Table 5.2 - TGA results of neat and filled TPU.

	T_{d1}(ºC)	$DTG1_{max}$(ºC)	T_{d2}(ºC)	$DTG2_{max}$(ºC)
TPU	191.8	229.7	342.1	380.0
TPU+HSCB	188.8	218.7	354.3	379.8
TPU+CNF	195.7	222.1	307.7	361.5
TPU+NS	185.4	219.6	358.0	378.8
TPU+NC	198.4	302.8	360.7	380.9
TPU+VCC	193.8	275.7	358.3	378.2
TPU+VCE	197.3	266.5	337.1	371.0

As reported by many other researchers, the introduction of MMT layers can greatly improve the thermal properties of the polymer matrix. [6,15] In the 1st step, the T_{d1} of NS composites was lower than the neat TPU. This can be related to the degradation of the surface treatment of the NS filler. In the 2nd step, the barrier effect of the silica is higher, thus increasing T_{d1}. The barrier effect of the NC layers in the TPU thermal stability is seen in both thermo degradation steps. The TPU T_{d1} and T_{d2}. were both increased due to the interface interactions and the barrier effect of the platelet-like layered silicates, with a high surface area. TPU thermal stability was improved with VCC and VCE, as expected, but higher for the latter. In the 1st step, filled TPU show increases upon T_{d1} and $DTG1_{max}$, showing better thermal stability. In the 2nd step, the VCC composite shows higher T_{d2} than neat TPEs, caused by the high filler barrier and strong interaction [16] between fillers and TPU. However, the VCE composite presents reduced T_{d2} than neat TPU.

The TGA results for SBS composites are shown in Table 5.3. HSCB and NS had a negative effect on thermal stability of SBS with a small drop on T_{d1} and more notorious reduction on T_{d2}. Similar to TPU, the strong barrier effect of the NC layers in the SBS thermal stability is also seen in both thermal degradation steps. The introduction of a well-dispersed MMT can prevent the heat transport and then improve the thermal stability of the nanocomposites. [17] [12] As expected, SBS thermal stability was once again improved with VCC and VCE fillers. As for TPU, VCC filled SBS presents an increment upon T_{d1} and $DTG1_{max}$ and T_{d2} and $DTG2_{max}$. This is caused by the outstanding barrier and interaction between fillers and TPE. [16]

Table 5.3- TGA results of neat and filled SBS.

	T_{d1}(ºC)	$DTG1_{max}$(ºC)	T_{d2}(ºC)	$DTG2_{max}$(ºC)
SBS	181.7	226.5	415.2	441.1
SBS+HSCB	180.3	228.0	402.1	439.5
SBS+NS	178.8	224.1	404.7	436.4
SBS+NC	183.3	227.5	417.7	441.3
SBS+VCC	188.1	234.4	417.7	436.7
SBS+VCE	183.5	226.8	413.9	442.0

5.1.4.2. Differential scanning calorimetry, analysis DSC

DSC technique was used to investigate thermal transitions on heating and cooling of neat and filled TPE composites, allowing the evaluation of the effects of the micro- and nanoparticles on macromolecular mobility at T_g. The presence of fillers could not only modify T_g, but also could interfere on the melting and crystallization processes (for semi-crystalline polymers). Assessed thermal parameters are listed in Table 5.4 to 5.7. In order to eliminate samples thermal history, a 2nd melting sweep was performed. In this way, it is guaranteed that all specimens are tested in identical conditions.

DSC traces of 1st melting sweep of neat and TPEs composites are shown in Figures 5.28 a) and b), respectively. The data is listed on Table 5.4.and 5.5.

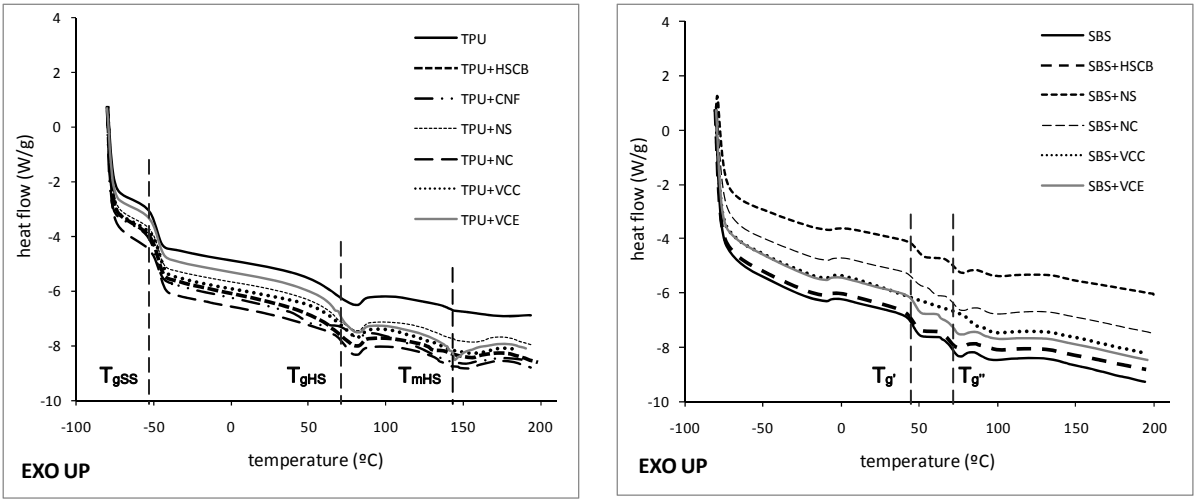

Figure 5.28 - Thermal transitions a) neat and TPU composites; b) neat and SBS composites (1st melting sweep).

Table 5.4 – Neat and filled TPU thermal transitions (1st melting sweep).

Sample	T_{gSS} (ºC)	T_{gHS} (ºC)	Onset poin t(ºC)	Tm_{HS} (ºC)	ΔH_{mHS} (J/g)	Onset point(ºC)	T_C (ºC)	ΔH_C (J/g)
TPU	-48.0	66.2	138.9	143.7	0.2	63.5	60.6	0.6
TPU+HSCB	-47.5	63.1	126.3	153.5	2.2	61.6	59.4	0.3
TPU+CNF	-48.0	76.7	120.4	152.6	3.5	63.8	60.7	0.5
TPU+NS	-47.1	67.0	130.0	145.2	3.1	64.1	57.0	0.6
TPU+NC	-45.9	74.0	128.9	155.1	3.9	59.7	55.7	0.5
TPU+VCC	-46.4	72.7	121.4	157.7	4.2	63.8	60.3	0.6
TPU+VCE	-47.2	70.3	140.5	158.4	4.0	63.5	60.5	0.5

The T_{gSS} of neat and filled TPU are around -48 °C.. The effect of micro- and nanoparticles incorporation in TPU is clearly seen on T_{gHS} values, where all fillers, with the exception of HSCB, showed a significant increase. The fillers incorporation had also increased HS melting temperature (T_{mHS}), the melting enthalpy (ΔH_{mHS}) (this latter implies an increment upon the degree of crystallinity). These changes in the crystallization lead to changes in the mechanical properties. An increase on the crystallinity degree would also explain the achieved mechanical properties. CNF, NC, and VC fillers have the highest effect in the TPU thermal transitions. As reported elsewhere, these fillers greatly improve, among others, the thermal stability. [10,18,19,20]

These results are in agreement with TGA analysis, where these fillers had the highest influence upon the thermal stability of the TPU hard segment domains.

Table 5.5 - Neat and filled SBS thermal transitions (1st melting sweep).

Sample	$T_{g'}$ (ºC)	$T_{g''}$ (ºC)
SBS	46.1	71.1
SBS+HSCB	46.1	69.8
SBS+NS	48.2	72.2
SBS+NC	46.3	72.5
SBS+VCC	82.5	92.9
SBS+VCE	47.1	72.9

The T_{gSS} of SBS was expected at -80 °C, but was not possible to detect it. The T_{gHS} of SBS is expected around 90°C, corresponding to PS domains. As can be observed in Figure 5.28b), a series of convoluted peaks appears on DSC trace between 50 and 100 °C, refered as $T_{g'}$ and $T_{g''}$. These peaks may correspond to several enthalpic relaxations of rich-phase HS domains. The presence of fillers seems to enhance these relaxations. Because polystyrene T_g appears in a series of convoluted peaks (Figure 5.28b)), a 2nd melting sweep was considered in order to eliminate samples thermal history and assess filler effect.

DSC traces of 2nd melting sweep of neat TPEs and its composites are shown in Figures 5.29 a) and b). Data is listed in Table 5.6 and 5.7.

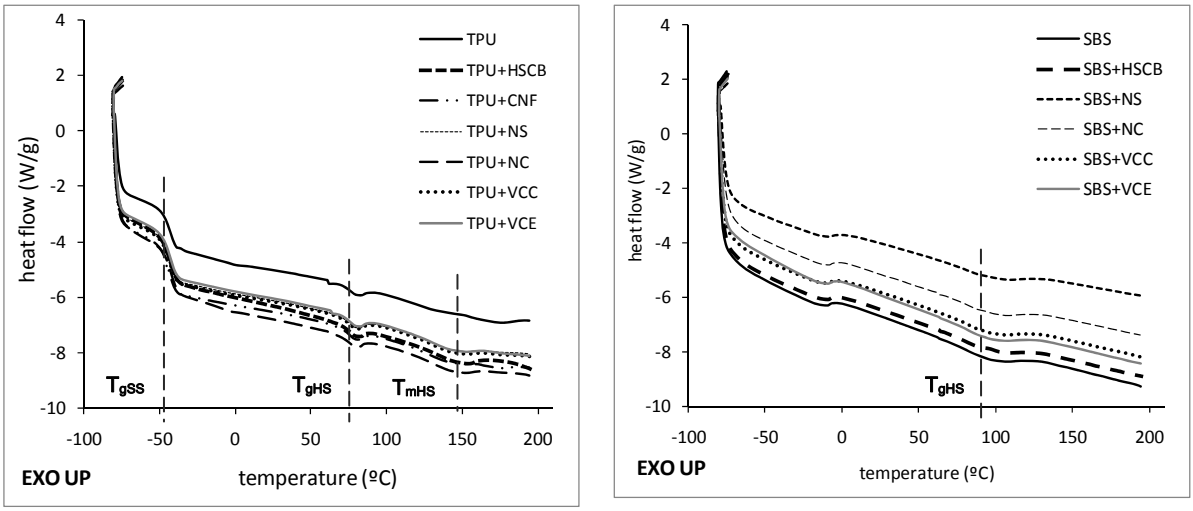

Figure 5.29 - Thermal transitions a) neat and TPU composites; b) neat and SBS composites (2nd melting sweep).

For neat and filled TPU, T_{gSS} is around -43°C, slightly lower than in the 1st scan. No major changes in the T_{gSS} were registered. The effect of micro- and nanoparticles incorporation in the TPU is clearly seen on the increment of T_{mHS} and ΔH_{mHS}. Once again, CNF, NC and VC show a remarkably thermal enhancement, interacting with TPUs HS domains. But, for the TPU composites the 1st sweep evidences stronger thermal transitions as compared with 2dn sweep.

Table 5.6 - Neat and filled TPU thermal transitions (2nd melting sweep).

Sample	T_{gSS} (ºC)	T_{gHS} (ºC)	Onset poin t(ºC)	Tm_{HS} (ºC)	ΔH_{mHS} (J/g)
TPU	-43.12	77.1	120.77	143.37	0.25
TPU+HSCB	-42.71	76.5	125.86	145.78	1.96
TPU+CNF	-43.30	76.1	119.96	149.72	1.30
TPU+NS	-42.78	76.1	124.47	148.90	0.68
TPU+NC	-42.34	76.2	116.02	152.17	2.35
TPU+VCC	-42.75	76.7	121.30	151.94	1.56
TPU+VCE	-42.91	76.2	117.38	152.44	1.95

For SBS composites (Figure 5.29b) and Table 5.7), the 2nd melting sweep show a T_{gHS} around 80 °C, with little effect upon various filler incorporation.

Table 5.7 - Neat and filled SBS thermal transitions (2nd melting sweep).

Sample	T_{gHS} (ºC)
SBS	81.8
SBS+HSCB	80.7
SBS+NS	80.1
SBS+NC	82.7
SBS+VCC	81.7
SBS+VCE	81.6

5.1.4.3. Thermal Conductivity, λ_c

λ_c measurements of reinforced TPEs showed no significant changes with filler incorporation (Figure 5.30). But still with only 1%wt. of fillers addition, a slight increase on the TPU thermal properties was observed. The incorporation of HSCB, CNF, NC and VCE slightly increased λ_c . In the case of carbon nanoparticles, the filler had the ability of improving λ_c, allowing for a more uniform heating, as would be expected. Also a random orientation of fibers will give a balance of thermal properties in all directions. NC had a remarkable effect in TPU thermal conductivity. Thermal properties improvements of these fillers were once again demonstrated. It was not possible to obtain an accurate NS filled TPU result due to the very small red value. Probably, NS is decreasing TPU λ_c. VCC and VCE have different effects on the different TPEs. Only HSCB and VCC had a positive effect on the SBS λ_c. The reasons for these differences can be found in geometrical and structural imperfections of the material at different levels of magnification [21] and the polymers nature.

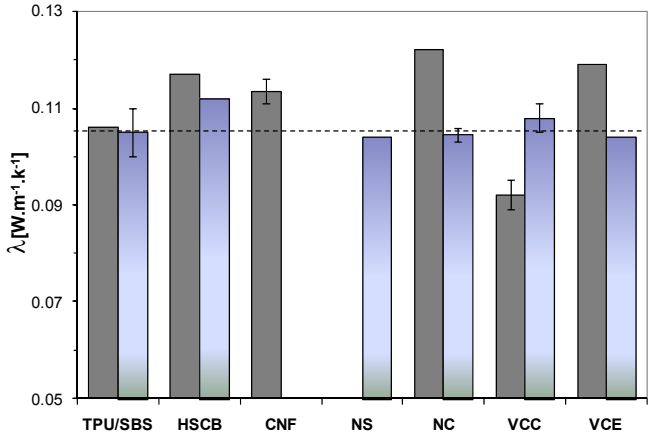

Figure 5.30 - Thermal Conductivity [$W.m^{-1}.k^{-1}$] measurements of micro- and nanoreinforced TPEs.

5.1.5. Flame resistance

Numerous studies have shown that the introduction of micro- and nanoparticles into polymers can greatly improve their properties such as flame resistance, reducing the heat released and improving fire retardancy. [20] Figure 5.31. show the variations of the linear burning rate, LBR, with filler addition for both TPEs. HSCB had greatly decreased TPEs linear burning rate. This enhancement is thought to be associated to a creation of carbon barrier that delays the combustion. NS also had a positive effect on both TPE composites. The CNF, NC and VCE particles had negative effect on the flammability of TPU.

SBS composites presents enhanced flame behavior with comparision with TPU. The thermal conductivity results reveals that SBS has a lower λ_c, but it is the particles incorporation that justifies the flame retardant behavior. VCs and NC show to be an inherent flame retardant material, with the SBS burning rate strongly decreasing. For burning, the availability of carbon and hydrogen is a pre-requisite [22]. Hydrogen and carbon group interactions with SBS have hindering the combustion process. These positive effect can limit the flame and heat diffusion of the substrate and act as an efficient protective barrier.[20] [15] The micro- and nanoparticles incorporation, VC and NC respectively, aim at minimizing the fire and its propagation risk, although, other particles achieved such an effect.

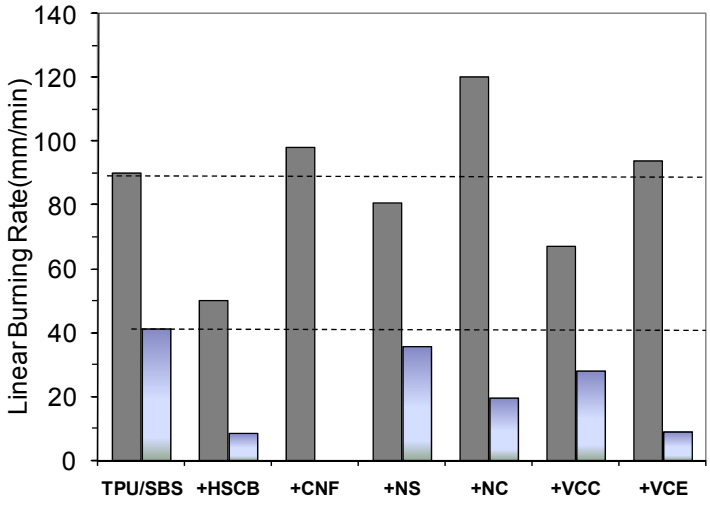

Figure 5.31- Linear Burning Rate of micro- and nanoreinforced TPEs.

5.1.6. Electrical Resistivity Measurements

Figura 5.31a) and b) shows how the values of surface resistivity and volume electrical conductivity change with the different nanofillers with the same wt.% of incorporation. Table 5.8 resumes main values.

Table 5.8 - Surface and volume electrical resistance measurements.

	TPU	TPU+HSCB	TPU+CNF	SBS	SBS+HSCB
Res. sup.(Ohm)	5.00E+11	1.20E+11	6.00E+09	1.00E+14	6.00E+10
Res. vol.(Ohm.m)	3.00E+14	7.85E+08	2.09E+07	1.00E+13	7.85E+06

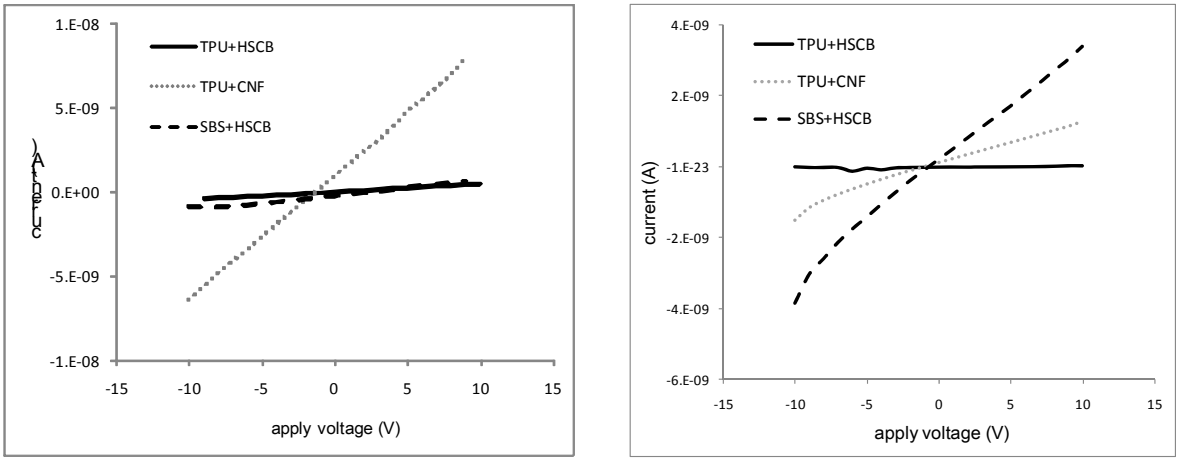

a) b)

Figure 5.32- Electrical measurement: a) Surface; b) Volume.

Aggregates may generate connected pathway of nanofiller, forming a conducting network for the nanocomposites [23] and electrical resistivity is reduced. But as observed in SEM images for HSCB and CNF composites (Figure 5.9 a) and b) and Figure 5.11) both they have a high level of dispersion being difficult to establish a conductive networks. This explains why there wasn´t any significant improvement in electrical conductivity for the level of incorporation. The presence of agglomerates becomes more important, as it was noted by Sandler et al. [24] in the case of carbon nanotubes dispersed in epoxy resin. [25] Although, with such a small amount of conductive fillers TPE shows a small drop in electrical resistance (Table 5.7). The exception to this is TPU+HSCB that shows a surface resistivity with the same order of magnitude of the TPU. All the other composites have their electrical resistivity decreased. This can be attributed to surface chemistry of the graphitic structure of the carbon material and differences in TPE nature. Note that TPU is amorphous and semi-crystalline one, and SBS is completely amorphous. Carbon composites of amorphous and semi-crystalline polymers have different electrical conduction behavior. [3,26]

5.2.REFERENCES

1. Pattanayak A., Jana S.C. - High-strength and low-stiffness composites of nanoclay-filled thermoplastic polyurethanes. Polymer Engineering & Science. Vol. 45: nº 11 (2005), p. 1532-1539.
2. Xanthos M. - Functional fillers for plastics. Weinheim: WILEY-VCH Verlag GmbH & Co KGaA, 2005.
3. Zhang Q-X., Yu Z-Z., Xie X-L., Mai Y-W. - Crystallization and impact energy of polypropylene/CaCO3 nanocomposites with nonionic modifier. Polymer. Vol. 45: nº 17 (2004), p. 5985-5994.
4. Aso O., Eguiazábal J.I., Nazábal J. - The influence of surface modification on the structure and properties of a nanosilica filled thermoplastic elastomer. Composites Science and Technology. Vol. 67: nº13 (2007), p. 2854-2863.
5. Breuer O., Sundararaj U. Polymer Composites. Vol. 25 (2004), p. 630.
6. Han B., Cheng A., Ji G., Wu S., Shen J. - Effect of organophilic montmorillonite on polyurethane/montmorillonite nanocomposites. Journal of Applied Polymer Science. Vol. 91: nº4 (2004), p. 2536-2542.
7. Lietz S., Yang J-L., Bosch E., Sandler J.K.W., Zhang Z., Altstädt V.- Improvement of the Mechanical Properties and Creep Resistance of SBS Block Copolymers by Nanoclay Fillers. Macromolecular Materials and Engineering. Vol. 292: nº 1 (2007), p. 23-32.
8. Soares B.G., Gubbels F., Jerome R.; Vanlathem E., Deltour R. - Electrical conductivity of polystyrene-rubber blends loaded with carbon black. American Chemical Society. Akron, OH, ETATS-UNIS (1928) (Revue). Vol.70: nº 1 (1997), pp. 146-172 (14 ref.): p. 60-70.
9. Zoran S.P., Javni I., Waddon A., Bánhegyi G. - Structure and properties of polyurethane-silica nanocomposites. Journal of Applied Polymer Science. Vol. 76: nº2 (2000), p. 133-151.
10. Xia H., Song M. - Preparation and characterization of polyurethane–carbon nanotube composites. Soft Matter. Vol. 1 (2005), p. 386 - 394.
11. Petrovic Z.S., Zavargo Z., Flynn J.H., Macknight W.J. - Journal of Applied Polymer Science. Vol. 51 (1994), p. 1087.
12. Chuang F.S., Tsen W.C., Shu Y.C. Polym. Degrad. Stab.Vol. 84 (2004), p.69.
13. Hwang J., Muth J., Ghosh T. - Electrical and mechanical properties of carbon-black-filled, electrospun nanocomposite fiber webs. Journal of Applied Polymer Science. Vol. 104: nº 4 (2007), p. 2410-2417.

14. Huxtable S.T., Cahill D.G., Shenogin S., Xue L., Ozisik R., Barone P., Usrey M. L.; Strano M. S., Siddons G., Shim M., Keblinski P. Nat. Mater. Vol.2 (2003), p. 731.

15. Vaia K. H., Giannelis E. P. Macromolecules. Vol. 30 (1997), p. 8000.

16. Zou H., Ran Q., Wu S., Shen J. - Study of nanocomposites prepared by melt blending TPU and montmorillonite. Polymer Composites. Vol. 29:n°4 (2008), p. 385-389.

17. Tortora M., Gorrasi G., Vittoria V., Galli G., Ritrovati S., Chiellini E. - Structural characterization and transport properties of organically modified montmorillonite/polyurethane nanocomposites. Polymer. Vol. 4323 (2002), p. 6147-6157.

18. Patil N.V. - Nanoclays make polymers stronger: polymer clay nanocomposites considerably increase the mechanical and thermal properties of polymers. In Advanced Materials & Processes. December 1, 2005. p. 39-40.

19. Chen Z., Gong K. - Preparation and dynamic mechanical properties of poly(styrene-<I>b</I>-butadiene)-modified clay nanocomposites. Journal of Applied Polymer Science. Vol. 84: n°8 (2002), p. 1499-1503.

20. Wang Z-Y, Han E.-H., Ke W. - Fire-resistant effect of nanoclay on intumescent nanocomposite coatings. Journal of Applied Polymer Science. Vol. 103: n°3 (2007), p. 1681-1689.

21. Friedrich K. - Mesoscopic aspects of polymer composites: Processing, structure and properties. Journal of Materials Science. Vol. 33: n° 23 (1998), p. 5535-5556.

22. RAMARAJ B. - Electrical and mechanical properties of thermoplastic polyurethane and polytetrafluoroethylene powder composites. Taylor & Francis. Vol. 46 (2007), p. 575-578.

23. Pötschke P., LIN B., Uttandaraman S. - Melt Mixing of Polycarbonate with Multi-Walled Carbon Nanotubes in Miniature Mixers. Macromolecular Materials and Engineering. Vol. 291: n°3 (2006), p. 227-238.

24. Sandler J., Shaffer M.S. P., Prasse T., Bauhofer W., Schulte K., Windle A. H. - Development of a dispersion process for carbon nanotubes in an epoxy matrix and the resulting electrical properties. Polymer Engineering and Science.Vol. 40 (1999), p. 5967-5971.

25. Schueler R., Petermann J., Schulte K., Wentzel H-P. - Agglomeration and electrical percolation behavior of carbon black dispersed in epoxy resin. Journal of Applied Polymer Science. Vol. 63: n°13 (1997), p. 1741-1746.

26. Krupa I., Chodak I. - Physical properties of thermoplastic/graphite composites. European Polymer Journal. Vol. 37 (2001), p. 2159-2168.

27. Canevarolo S.V. - Técnicas de Caracterização de Polímeros. 2003, São Paulo: Artliber Editora.

CHAPER 6

CONCLUSIONS AND FUTURE WORK

The thoroughly characterization analysis carried out on chapter 5 are combined to establish the relationships between the fillers, morphology and overall performance of the investigated micro- and nanocomposites. Some guidelines regarding the potential research and development work that can be made in the study of thesis composites are given at the end.

6.1. CONCLUSIONS

The present work covers a study focused on the attempt to obtain a micro- and nanofilled polymer composite with superior properties. A Polyurethane (TPU) and a Styrene-Butadiene-Styrene (SBS) based thermoplastic elastomers were mixed with micronized (crude and exfoliated vermiculite) and nanosized (nanoclay, nanosilica, high-structured carbon black and carbon nanofibers) reinforcing particles in 1 %wt. of incorporation, using a laboratory-scale mixing mini-device, and the same processing conditions.

The importance of mixing in polymer processing is undeniable. The thoroughly characterization allows inferring that the attempts to disperse these fillers in a viscous material such as polymer is difficult, but crucial for grant enhanced properties by the micro- and nanoparticles incorporation in the polymers matrix.

Good dispersion, adhesion and a randomly particles orientation in TPE matrix for most cases were possible to obtain by the adopted mixing procedure. Laboratory-scale mixing mini-device offers a powerful tool for processing composites and proved to be useful in dealing with materials of such difficult exfoliation and dispersion abilities.

Morphology, mechanical, thermal and flame retardant properties and electrical resistivity were assessed. The results of the experiments presented here showed improvements upon the system performance and added functionalities of TPE. Polymer morphology play a key role in final assessed properties. Face to the obtain results, it was demonstrated that preparations method, chemical nature of pure polymer, chemical nature of the particle, particle size and distribution, their tendency to aggregate in the organic matrix on account of their high surface energy, all these aspects strongly influence the final morphology of the nanocomposites and therefore its performance. It was shown that different type of nanoparticles exhibited different influences on the properties of nanofilled TPE, also depending upon the type of TPE.

Fillers have induced promising improvements in nanocomposites mechanical performance, with greater influence on the TPU mechanical and thermal properties. Nanofilled TPU show significant improvement upon the stress and strain at break. Higher tensile properties becomes from the fillers dispersion, on the nanometer scale and strong interaction between the micro- and nanoparticles and polymer matrix.
Clearly the, TGA and DSC results have showed that the micro- and nanoparticles have a great effect on the composites thermal properties.

Fillers incorporation had no notorious effect on SBS mechanical properties. The nanoreinforced SBS present always lower tensile modulus, same deformability but enhanced flame behavior. SBS Nanocomposites showed to be very sensitive to the shape/size of the incorporated nanofillers.
Fillers low content is a very important aspect in composites composition, not only because lower concentrations reduces composites prices, but also for the problem of minimization caused by an excess of the filler in the mechanical properties of the final composite. The nanocarbon black fillers have decreased TPEs electrical resistivity. Carbon nanofillers also positively influenced mechanical and thermal properties.

Overall, experimental results have provided a fundamental understanding of the fillers contributing factors.

6.2. FUTURE WORK

We aim in future work at:

- Studying the deformation mechanisms of TPE nanocomposites, namely the effect of nanofillers on deformation capabilities in a way of unraveling the factors underlying the mechanical characteristics, the dispersion and adherence relationship.
- Establishing the relationships between mechanical deformation and electrical resistivity in TPE nanocomposites.

APPENDIX I

Thermoplastic Elastomers Data Sheet

APPENDIX II

Micro- and Nanosize Fillers Data Sheet

APPENDIX III

TPE Composites FTIR Spectra

III. Fourier transform infrared spectroscopy, FTIR

Principal neat and TPEs composite functional groups and the main peaks were assigned (Figure III.1 and III.2). No new absorption bands were observed, but existing bands intensity has increased, demonstrating some degree of interaction between fillers and polymers matrix.

In Figure III.1 is shown the spectra for TPU composites. The peak around 3390 cm^{-1} and 1536 cm^{-1} was attributed to stretching vibration of amine groups N-H, which is due to the hydrogen bonded -NH in the urethane linkage. Carbonyl -C=O stretching are shown at 1730 cm^{-1} which are considered to be free and hydrogen bonded carbonyls. The absorption bands around 2964 cm^{-1} were attributed to the asymmetric and symmetric stretching vibration of methylene CH_2. Peak 1602 cm^{-1} is attributed to C=C group and 905 cm^{-1} to C-O bonded.

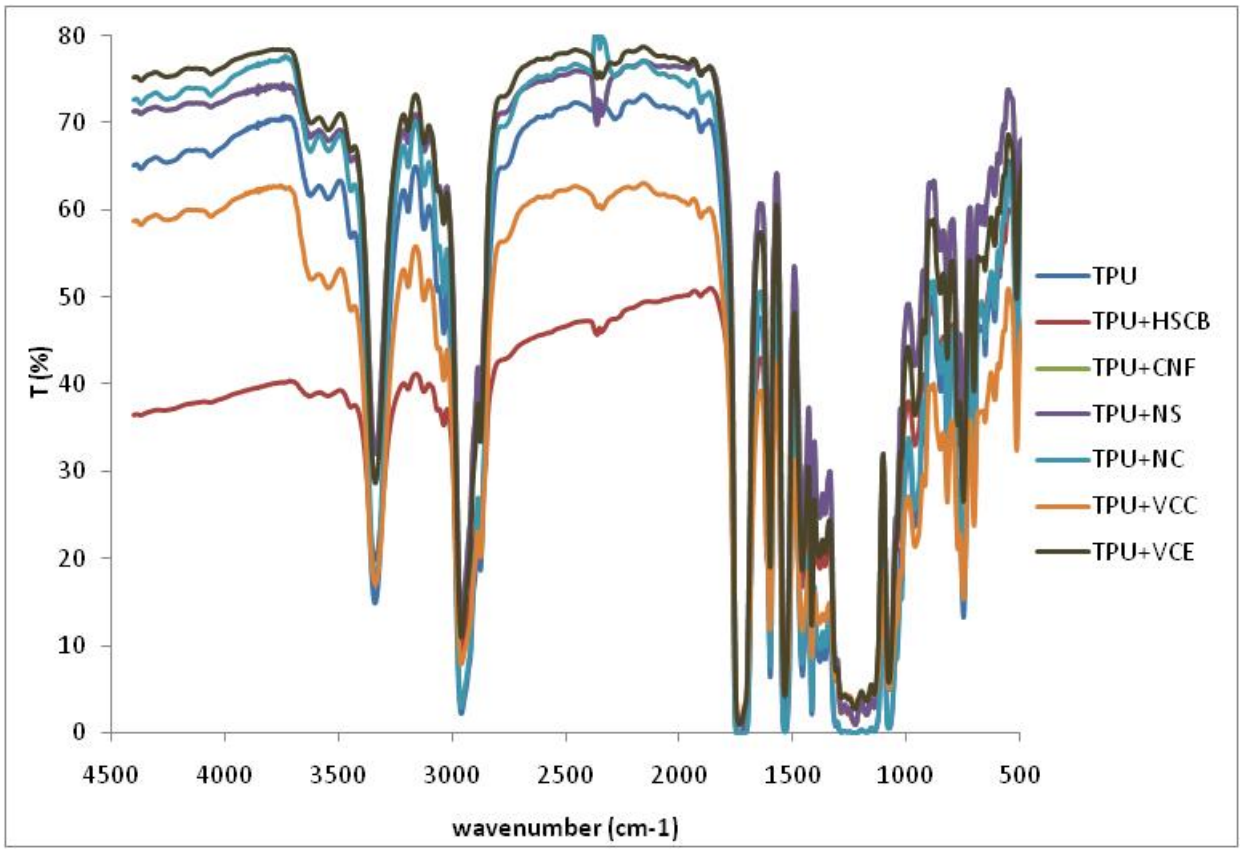

Figure III.1 - FTIR Spectra of neat and TPU composites.

In Figure III.2 is shown the spectra for SBS composites. The bands at 2922 cm^{-1}, 1456 cm^{-1} and 700 cm^{-1} was attributed to stretching vibration of C-H band. The absorption bands around 1642 cm^{-1} were attributed to stretching vibration of C=C.

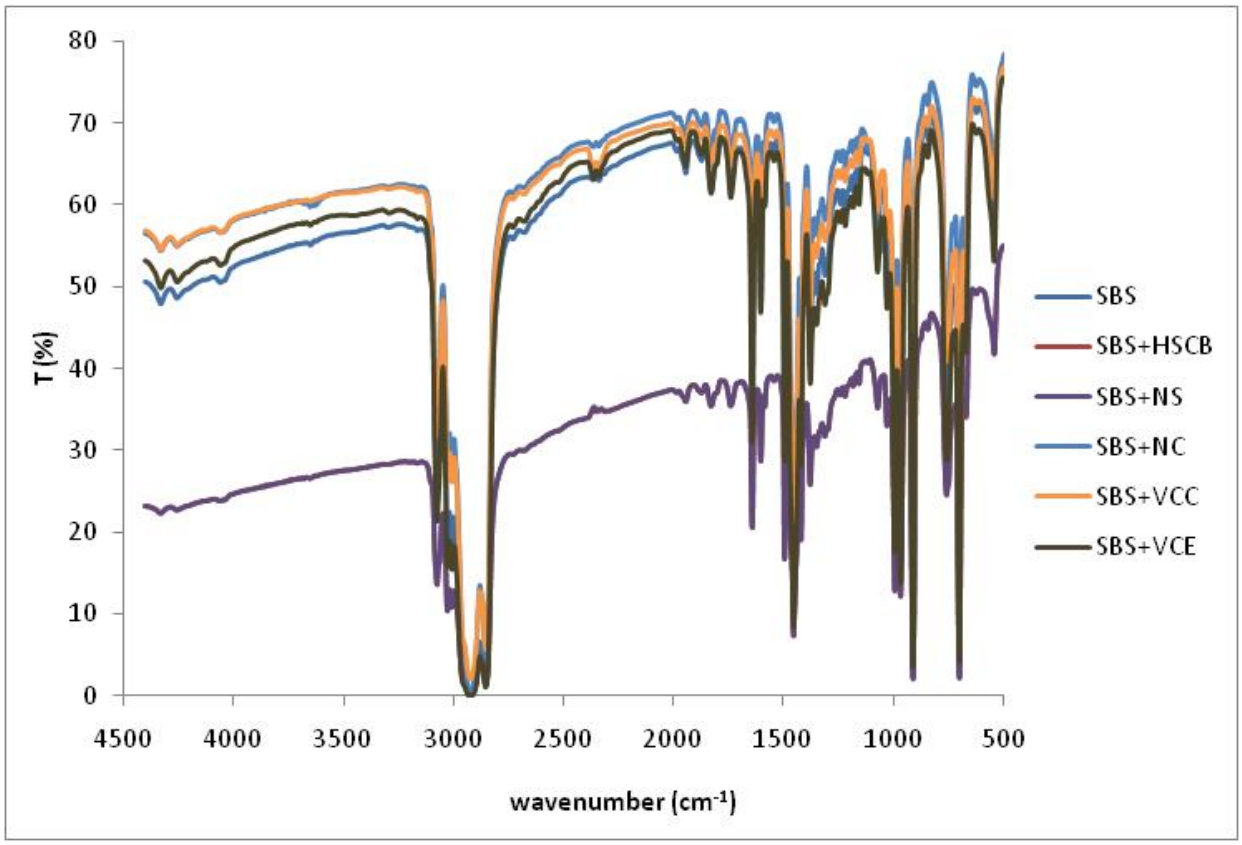

Figure III.21- FTIR Spectra of neat and SBS composites.

APPENDIX IV

Yield Energy and Energy at Break Results

of TPE Composites

IV.1.Energy results

In Figure IV.1 and IV.2 are shown the effect of micro- and nanoparticles on the TPEs yield energy, U_y, and energy at break, U_b.

With the exception of high structure carbon black (HSCB) carbon nanofibers (CNF) and crude vermiculite (VCC) fillers, the U_y of TPU decreased with the presence of micro- and nanofillers (Figure IV.1). CNF had no effect on TPU U_y. All fillers with the exception of HSCB had a negative effect on the SBS U_y.

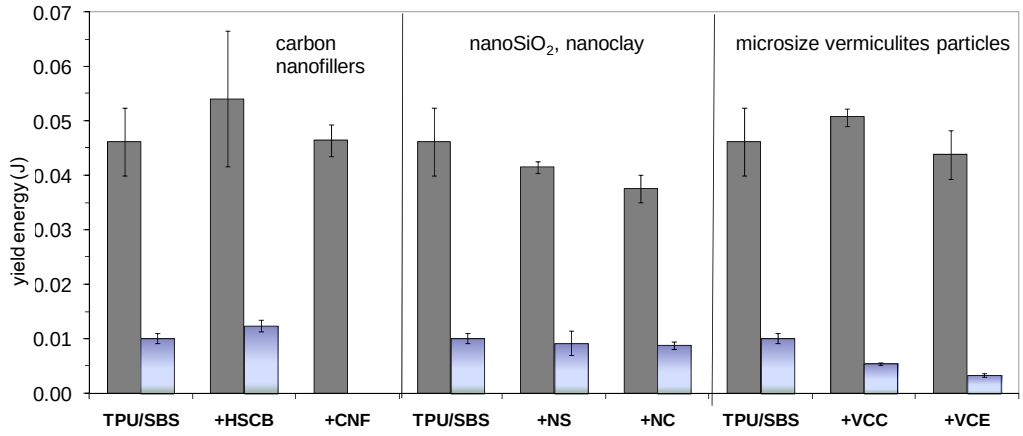

Figure IV.1 - Yield energy, U_y.

The TPU composites had significant improvements upon the U_b. The HSCB, CNF, nanosilica (NS), nanoclay (NC) and the vermiculites (VC) incorporation increased the U_b . with the most notorious effect observed on the TPU filled with NS (Figure IV.2).

With the exception of VC fillers, the U_b of SBS improved with the presence of nanofiller particles (Figure IV.2). The VC fillers have affected negatively the SBS U_b, and it is thought to be associated to the formed microsized particles.

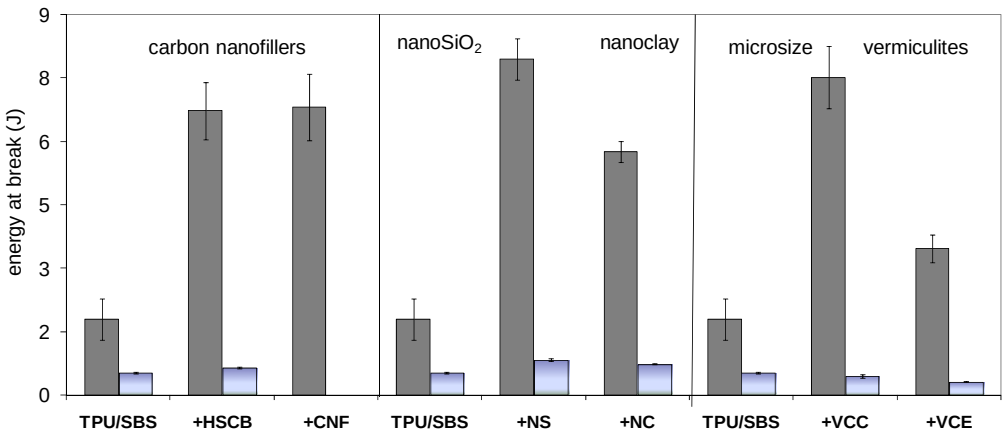

Figure IV.2 – Energy at break, U_b.